Coral Reefs
August 2020, Volume 39 Issue 4 Pages 1001-1025
https://doi.org/10.1007/s00338-020-01924-8
https://archimer.ifremer.fr/doc/00623/73501/

Towards a rigorous species delimitation framework for scleractinian corals based on RAD sequencing: the case study of Leptastrea from the Indo-Pacific

Arrigoni Roberto [1, 2, 3, *] , Berumen Michael L. [2], Mariappan Kiruthiga G. [2], Beck Pieter S. A. [3], Hulver Ann Marie [2], Montano Simone [4, 5], Pichon Michel [6], Strona Giovanni [7], Terraneo Tullia Isotta [2, 8], Benzoni Francesca [2]

[1] Department of Biology and Evolution of Marine Organisms (BEOM), Stazione Zoologica Anton Dohrn Napoli, Villa Comunale, 80121, Naples, Italy
[2] Red Sea Research Center, Division of Biological and Environmental Science and Engineering, King Abdullah University of Science and Technology, Thuwal, 23955-6900, Saudi Arabia
[3] European Commission, Joint Research Centre (JRC), Ispra, Italy
[4] Dipartimento Di Scienze Dell'Ambiente E del Territorio, Università Degli Studi Di Milano-Bicocca, Piazza della Scienza 1, 20126, Milan, Italy
[5] Marine Research and High Education Center, Magoodhoo Island, Faafu Atoll, Maldives
[6] Queensland Museum, Biodiversity and Geosciences, Townsville, QLD, 4810, Australia
[7] Research Centre for Ecological Change, University of Finland, 00014, Helsinki, Finland
[8] ARC Centre of Excellence for Coral Reef Studies, James Cook University, Townsville, QLD, 4810, Australia

* Corresponding author : Roberto Arrigoni, email address : roberto.arrigoni@szn.it

Abstract :

Accurate delimitation of species and their relationships is a fundamental issue in evolutionary biology and taxonomy and provides essential implications for conservation management. Scleractinian corals are difficult to identify because of their ecophenotypic and geographic variation and their morphological plasticity. Furthermore, phylogenies based on traditional loci are often unresolved at the species level because of uninformative loci. Here, we attempted to resolve these issues and proposed a consistent species definition method for corals by applying the genome-wide technique Restriction-site Associated DNA sequencing (RADseq) to investigate phylogenetic relationships and species delimitation within the genus Leptastrea. We collected 77 colonies from nine localities of the Indo-Pacific and subjected them to genomic analyses. Based on de novo clustering, we obtained 44,162 SNPs (3701 loci) from the holobiont dataset and 62,728 SNPs (9573 loci) from the reads that map to coral transcriptome to reconstruct a robust phylogenetic hypothesis of the genus. Moreover, nearly complete mitochondrial genomes and ribosomal DNA arrays were retrieved by reference mapping. We combined concatenation-based phylogenetic analyses with coalescent-based species tree and species delimitation methods. Phylogenies suggest the presence of six distinct species, three corresponding to known taxa, namely Leptastrea bottae, Leptastrea inaequalis, Leptastrea transversa, one characterized by a remarkable skeletal variability encompassing the typical morphologies of Leptastrea purpurea and Leptastrea pruinosa, and

two distinct and currently undescribed species. Therefore, based on the combination of genomic, morphological, morphometric, and distributional data, we herein described Leptastrea gibbosa sp. n. from the Pacific Ocean and Leptastrea magaloni sp. n. from the southwestern Indian Ocean and formally considered L. pruinosa as a junior synonym of L. purpurea. Notably, mitogenomes and rDNA yielded a concordant yet less resolved phylogeny reconstruction compared to the ones based on SNPs. This aspect demonstrates the strength and utility of RADseq technology for disentangling species boundaries in closely related species and in a challenging group such as scleractinian corals.

Keywords : ezRAD, dDocent, Holobiont, SNAPP, Bayes factor delimitation, Morphometrics, New species

Introduction

Scleractinian corals represent the major bioconstructors of tropical coral reefs, with millions of species living in closely association with them, and support economies of several countires (Knowlton 2001; Roberts et al. 2002). Nevertheless, they are threatened organisms given their rapid decline worldwide in response to numerous enthropogenic drivers both at local and global scales (Pratchett et al. 2017; Hughes et al. 2018, 2019). Considering this ongoing loss of coral diversity and the high extinction rate in marine habitats as we are transitioning in the Anthropocene era (McCauley et al. 2015; Hughes et al. 2017; Johnson et al. 2017), conservation strategies urgently call for accurate species assessments in characterizating coral biodiversity.

Coral species have been traditionally described using morphological traits of skeleton (Wells 1956; Chevalier 1975). Disagreements between conventional- and genetics-based systematics are common in all genera and have left the delineation of most extant species unresolved (Kitahara et al. 2016). From a molecular perspective, currently available markers are insufficient for species delimitation in the majority of genera (see for example Forsman et al. 2009; Terraneo et al. 2016). Mitochondrial barcoding genes of Anthozoa exhibit a slow evolutionary rate (Shearer et al. 2002; Hellberg 2006) while the nuclear ITS marker poses problems as it displays elevated intraindividual and

intraspecific variation and retention of ancient lineages (Van Oppen et al. 2000; Vollmer and Palumbi 2004). From a morphological point of view, environment-induced phenotypic plasticity (Todd 2008; Paz-García et al. 2015) and genotype-driven intraspecific morphological variation (Carlon and Budd 2002; Dimond et al. 2017) have contributed to the taxonomic uncertainties. Furthermore, evolutionary convergence, morphological stasis, and homoplasy occur in several traditional skeletal traits (Fukami et al. 2008; Flot et al. 2011; Arrigoni et al. 2016a, 2019).

The advent of high-throughput sequencing technologies provides an unprecedented chance to access a huge amount of genomic information and to resolve controversial phylogenetic relationships in great depth and all taxonomic levels (Metzker 2010). This is particularly true for Restriction-site associated DNA sequencing (RADseq; Miller et al. 2007; Baird et al. 2008), a reduced-genome technique that can be applied to non-model organisms for which there are no reference genome data available (Davey and Blaxter 2010). This approach relies on the sequencing of short DNA fragments flanking restriction sites, generating hundreds to thousands of random, unlinked, and homologous genomic loci, and single nucleotide polymorphisms (SNPs) (Andrews et al. 2016). Typically, RADseq has been used to establish phylogenetic relationships between closely related species and populations (Rubin et al. 2012; Ceballos et al. 2019). Nevertheless, its application has been successfully extended from shallow timescales also to divergences dating back to 50–60 Ma (Cariou et al. 2013; Eaton et al. 2017).

In this work, the scleractinian genus *Leptastrea* Milne Edwards and Haime, 1849, actually transferred to *Incertae Sedis* at the family level (Budd et al. 2012), is selected as case study to propose a rigorous integrative method to infer evolutionary relationships and delimitation of species within hard corals. *Leptastrea* is widely distributed throughout the Indian and central Pacific Ocean, where it is a common element of shallow reefs (Veron 2000). The genus currently includes seven colonial and zooxanthellate extant nominal species (Hoeksema and Cairns 2019), namely *L. aequalis* Veron, 2000, *L. bewickensis* Veron, Pichon and Best, 1977, *L. bottae* (Milne Edwards and Haime, 1849), *L. inaequalis* Klunzinger, 1879, *L. purpurea* (Dana, 1846), *L. pruinosa* Crossland, 1952, and *L. transversa* Klunzinger, 1879. According to the distribution maps in Veron (2000), they are widely distributed from the Red Sea to the central Pacific with the exception of *L. bewickensis* spanning from the eastern Indian to the Central Pacific. Species ascribed to *Leptastrea* have been described exclusively based on size and shape of skeletal structures (Matthai 1914; Chevalier 1975; Scheer and Pillai 1983). Nevertheless, remarkable morphological variation of the skeleton was described for species such as *L. bottae*, *L. purpurea*, and *L. transversa* from distinct habitats or different localities of the Indo-Pacific (Matthai 1914; Chevalier 1975; Veron et al. 1977; Scheer and Pillai 1983). Such variability has led to the

85 complex synonymy history of, for example, *L. purpurea* with several nominal species described starting from the 19th
86 century and now considered its junior synonyms (Milne Edwards and Haime1849; Verrill 1867; Hoeksema and Cairns
87 2019). Moreover, some species can be superficially so similar that taxonomists have hesitated to tell them apart, *e.g.*
88 *L. purpurea* with *L. transversa* and *L. purpurea* with *L. pruinosa* (Vaughan 1918; Scheer and Pillai 1974; Veron et al.
89 1977). Due to the challenges of its species morphological identification, and the resulting taxonomic uncertainty,
90 *Leptastrea* provides a good case study to address evolutionary and systematics issues in scleractinians. It has, however,
91 remained poorly studied without any genetic analyses aimed to clarify species boundaries carried out so far (Fukami
92 et al. 2008; Arrigoni et al. 2012). Therefore, *Leptastrea* is an ideal model to test general questions that are frequently
93 applied to most phylogenetic studies on corals: (a) how can we distinguish closely related and morphologically similar
94 species?; (b) which morphological characters are diagnostic of the independently evolving molecular lineages (*i.e.*
95 species)?; (c) what is the actual species geographic distribution?
96 Herein, we applied a genome-scale ezRAD framework (Toonen et al. 2013) to elucidate the phylogenetic
97 relationships and species delimitation in *Leptastrea*, using one of the largest coral genomic datasets published so far
98 from a large geographic range spanning the whole Indo-Pacific. We newly sequenced and assembled three
99 phylogenomic datasets: (a) 9,573 loci from the coral dataset by mapping reads to coral transcriptome reference; (b)
100 3,701 anonymous loci from the holobiont dataset (a close association of a diverse variety of organisms including coral,
101 obligate symbiotic dinoflagellate algae, bacteria, fungi, and microbes, see Forsman et al. 2017) based on *de novo*
102 assembly; (c) nearly complete mitochondrial genomes and ribosomal DNA arrays, including the barcoding region of
103 the cytochrome oxidase subunit I gene and the ITS1 and ITS2 regions traditionally used in coral phylogenetic work,
104 respectively. Phylogenomic information was then combined with morphological, morphometric, and geographical
105 data to propose species delineation of *Leptastrea* in an integrative taxonomic context arising from multiple lines of
106 evidence.
107
108 **Materials and methods**
109 **Sampling and identification**
110 A total of 77 *Leptastrea* colonies were sampled while SCUBA diving between 1 and 35 m depth at nine Indo-
111 Pacific localities, namely Saudi Arabia (Red Sea coast), Djibouti, Yemen (Gulf of Aden coast and Socotra Island),
112 Madagascar, Mayotte Island, the Maldives, Papua New Guinea, New Caledonia, and French Polynesia (Data S1). Two

113 *Lobactis scutaria* (Lamarck, 1801) from the Red Sea were used as outgroup because this species is phylogenetically
114 closely related to *Leptastrea* (Fukami et al. 2008; Arrigoni et al. 2012) and its transcriptome is available (Kitchen et
115 al. 2015). Digital images of living corals were taken in the field with a Canon Powershot G9 in an Ikelite underwater
116 housing system. Samples were broken off from the colonies with hammer and chisel. A small fragment of each sample
117 was then preserved in 96% ethanol or CHAOS solution (not an acronym; 4 M guanidine thiocyanate, 0.1% N-lauroyl
118 sarcosine sodium, 10 mM Tris pH 8, 0.1 M 2-mercaptoethanol) (Sargent et al. 1986) for molecular analyses. The
119 remaining portion of the corallum was immersed in sodium hypochlorite for 48 hours to remove all soft parts, rinsed
120 in freshwater, and dried for identification and microscope observation. Material sampled for this study was deposited
121 at King Abdullah University of Science and Technology (KAUST, Kingdom of Saudi Arabia), University of Milano-
122 Bicocca (UNIMIB, Italy), Institut de Recherche pour le Développement (IRD, New Caledonia), James Cook
123 University (JCU, Australia), and the Muséum National d'Historie Naturelle (MNHN, France). Specimens were
124 identified to species based on skeleton morphology following Milne Edwards and Haime (1849), Klunzinger (1879),
125 Crossland (1952), Veron et al. (1977), and Veron (2000) as well as referring to illustrations of holotypes in their
126 original descriptions. Moreover, the type specimens of *L. bottae*, *L. inaequalis*, *L. purpurea*, and *L. transversa* and
127 were examined (Figs. 1a, e, i, m, q) (Data S2).
128
129 **DNA extraction, ezRAD library preparation, and sequencing**
130 Total DNA was extracted using DNeasy® Blood and Tissue kit (Qiagen Inc., Hilden, Germany) for coral
131 fragments preserved in ethanol or through a phenol-chloroform based method for samples in CHAOS. A Qubit®
132 Fluorometer 3.0 (Thermo Fisher Scientific Inc., Waltham, MA, USA) was used to check that each DNA extract
133 contained a minimum of 1.2-1.3 µg of genomic DNA. We followed protocols by Toonen et al. (2013) and Knapp et
134 al. (2016) for DNA digestion and ezRAD library preparation. Each sample was digested using frequent cutter
135 restriction enzymes MboI and Sau3AI (New England BioLabs, Ipswich, MA, USA) to cleave sequences at GATC cut
136 sites (Toonen et al. 2013). All ezRAD libraries were obtained using TruSeq Nano DNA HT Library Prep Kit (Illumina,
137 San Diego, CA, USA), size selected at 350 bp, ligated with a unique combination of Illumina adapters D701-D712
138 and D501-D508, normalized, and combined to two pools of 40 and 39 libraries, respectively. Each library pool was
139 run in a single 150 bp paired-end lane on Illumina HiSeq 4000 System at KAUST Genomics Core Lab (Thuwal,

Kingdom of Saudi Arabia). The sequenced lengths, number of reads, and sample information for each library are presented in Data S1.

ezRAD data processing

The Illumina raw data consisted of 509,354,215 million 150 bp reads for all 77 samples. All samples were de-multiplexed using their unique barcode and adapter sequences under the Illumina pipeline bcl2fastq/2.17.1.14 (with no mismatches allowed for the barcode), effectively removing reads that lacked identifiable barcode pairs. All samples were trimmed for low quality base-pairs and adapter sequences using Trimmomatic v.0.36 under the default parameters (Bolger et al. 2014). The ezRAD analysis was performed twice, first as a holobiont and after assembling the reads to the *L. scutaria* transcriptome.

To perform the holobiont analysis, the dDocent 2.2.25 pipeline mentioned in Puritz et al. (2014) was followed under the default parameters unless indicated here. Total reads were placed in a folder as *.F.fq.gz and *.R.fq.gz and trimmed reads were placed as *.R1.fq.gz and *.R2.fq.gz, respectively. About 5.9 million trimmed reads per sample were obtained. Briefly, the dDocent v.2.2.25 pipeline (Puritz et al. 2014) was started merging the trimmed reads using PEAR v.0.9.6 (Zhang et al. 2013) and an assembly was created using BWA v.0.7.15 (Li and Durbin 2009) under the following options, t 16 -a -M -T 10 –R. The bam files were then sorted and merged using SAMtools v.1.6 (Li et al. 2009) to create one single bam file. Variants were called using FreeBayes (Garrison and Marth 2012) under the following options, -0 -E 3 -G 5 -z 0.1 -X -u -n 4 --min-coverage 5 --min-repeat-entropy 1 -V –b options. The post-assembly dDocent 2.2.25 pipeline was done after aligning the trimmed reads to the transcriptome of *L. scutaria* using Bowtie v.2 2.3.4 (Langmead and Salzberg 2012), and the aligned reads were converted to fastq files using BEDTools v.2.26.0 (Quinlan and Hall 2010). These files were renamed as *F.fq.gz and *R.fq.gz and were placed along with the *L. scutaria* transcriptome as reference.fasta. dDocent 2.2.25 (Puritz et al. 2014) was initiated without the assembly option to create the reference fasta file and executed with the same options as mentioned above. SNPs were identified using FreeBayes (Garrison and Marth 2012) following Forsman et al. (2017).

One of the main benefits of ezRAD is that it ends up with both considerable vertical and horizontal coverages (as depth and breadth) (Terraneo et al. 2018a, 2018b; Stobie et al. 2019). While the former is used to call SNPs, the latter generates very long contigs, resulting in the resolution of the complete or a large percentage of the mitochondrial genomes and other multicopy gene regions such as ribosomes. Reference mapping against previously published

168 reference sequences of mitochondrial genome (mitogenome) and nuclear ribosomal DNA (rDNA, including the
169 complete 18S, ITS1, 5.8S, ITS2, and 28S regions) was carried out to acquire and compare nearly complete
170 mitogenomes and rDNA from each library. As reference, we used the complete mitochondrial genome of *Polycyathus*
171 *chaishanensis* Lin et al. 2012 (JF825140) and the nearly complete rDNA of *L. purpurea* (LT631161, HE648522,
172 JQ966138). Raw de-multiplexed reads were trimmed for adapters and low-quality bps using Trimmomatic v.0.36
173 (Bolger et al. 2014). Trimmed reads were aligned to the reference sequences using Bowtie v.2 2.3.4 (Langmead and
174 Salzberg 2012) in --fast-local mode. Aligned reads were convert to bam and indexed using SAMtools v.1.6 (Li et al.
175 2009), and the consensus sequences were identified using SAMtools mpileup combined with Vcfutils.pl.
176
177 **Phylogenomic analyses**
178 The resulting vcf files from both the coral and holobiont datasets were further filtered using VCFtools v.0.1.16
179 (Danecek et al. 2011). To examine the sensitivity of the phylogenetic inference to the filtering process, we generated
180 two filtered supermatrices for both the coral and holobiont datasets. In particular, following Forsman et al. (2017) we
181 obtained the "coral-max" and the "holobiont-max" supermatrices using the following filter options: mean depth = 5,
182 max missing data = 50%, and minimum distance between SNPs = 10. Conversely, we generated the "coral-min" and
183 the "holobiont-min" supermatrices using the following filter options: mean depth = 10, max missing data = 0%, and
184 minimum distance between SNPs = 300. Haplotypes were then called and filtered for complex loci, potential paralogs,
185 missing data, and sequencing errors using the rad_haplotyper v.1.1.8 pipeline
186 (https://github.com/chollenbeck/rad_haplotyper; Willis et al. 2017). Contigs were then collapsed into genotypes for
187 final analyses. PGDspider v.2.1.1.5 (Lischer and Excoffier 2011) was used to convert the dataset to the required file
188 types for further analysis. The resulting four concatenation-based loci supermatrices were analyzed in RAxML v8.2.10
189 (Stamatakis 2014) for maximum likelihood (ML) phylogenetic inference. We applied the GTR + GAMMA
190 substitution model for all the phylogenetic analyses, and the branch support was assessed by 500 rapid bootstrap
191 replicates. The "coral-max" and "holobiont-max" supermatrices were also investigated by means of Bayesian
192 Inference with BEAST v.2.5.2 (Bouckaert et al. 2014). The GTR + GAMMA substitution model and an uncorrelated
193 (lognormal) clock model were applied. Chains were run for 100 million iterations, sampling every 50,000 iterations,
194 and checked for stationarity and parameter effective sample sizes with Tracer v.1.7 (Rambaut et al. 2018). Final trees

were built using the BEAST module TreeAnnotator v.2.5.2 (Bouckaert et al. 2014), discarding the first 10% as burnin as indicated by Tracer v.1.7 (Rambaut et al. 2018).

The mitogenome and rDNA datasets were aligned using MAFFT v.7 with the E-INS-i strategy (Katoh and Standley 2013). We determined the optimal among-gene partitioning scheme and model choice for dataset in PartitionFinder v.2 (Lanfear et al. 2016) under the Bayesian Information Criterion (BIC). The mitogenomes were partitioned according to the genes, considering all intergenic regions as a single partition, while genes were further partitioned according to the codon positions. The rDNA dataset was partitioned in five partitions, 18S, ITS1, 5.8S, ITS2, and 28S. Phylogenetic relationships based on mitogenome and rDNA alignments were inferred using both ML and BI, under parameters and options applied for the "coral-max" and "holobiont-max" supermatrices. We also built ML phylogenetic trees based on two barcoding loci traditionally and widely used for scleractinian corals (Kitahara et al. 2016), namely a portion of the cytochrome oxidase subunit I gene of the mitochondrial genome (COI) and the complete ITS1, 5.8S, and ITS2 regions of the rDNA (ITS). *Lobactis scutaria* was selected as outgroup for all the phylogenetic analyses following Arrigoni et al. (2012). All ML and BI analyses were run on the CIPRES Science Gateway (Miller et al. 2010).

Species delimitation analyses

Bayes Factor Delimitation with genomic data (BFD*) was used to test eight reasonably possible species delimitation models (Leaché et al. 2014). In particular, we considered the following models: (1) one single species; (2) current taxonomy, distinguishing *L. bottae*, *L. inaequalis*, *L. pruinosa*, *L. purpurea*, *L. transversa*, and the undescribed morph from Madagascar and Mayotte (six species); (3) current taxonomy but lumping *L. purpurea* with *L. transversa* (five species); (4) current taxonomy but lumping *L. purpurea* with *L. pruinosa* and *L. transversa* (four species); (5) groups resulting from ezRAD phylogenies including the undescribed morph from Madagascar and Mayotte and *L.* cf *bottae* from New Caledonia and Papua New Guinea (six species); (6) proposed ezRAD phylogenies but splitting *L. purpurea* and *L pruinosa* (seven species); (7) proposed ezRAD phylogenies but lumping *L. purpurea* with *L pruinosa* and *L. transversa* (five species); (8) proposed mitogenome and rDNA phylogenies (five species). In order to reduce computational time, we sampled three individuals per species. We used VCFtools v.0.1.16 (Danecek et al. 2011) to generate a supermatrix of 21 individuals, including only unlinked biallelic SNPs with 0% missing data as required by SNAPP. The SNAPP package (Bryant et al. 2012) implemented in BEAST v.2.5.2 (Bouckaert et al.

223 2014) was used to run a path sampling method with 48 steps, each one consisting of 100,000 MCMC generations
224 saving every 1000 generations with a pre-burnin of 10,000 steps. Model convergence was assessed using Tracer v.1.7
225 (Rambaut et al. 2018). We compared and ranked models to select the best-supported species hypothesis by using the
226 estimated marginal likelihood (MLE) of each model and by calculating the Bayes factor (BF) as (2 * [model1 –
227 model2]) (Kass and Raftery 1995).
228 The species tree analysis was based on the results of BFD* runs described above, using the best supported model.
229 A coalescent-based species tree was obtained by using the SNAPP package (Bryant et al. 2012) implemented in
230 BEAST v.2.5.2 (Bouckaert et al. 2014). In order to reduce the complexity in species tree estimation and increase
231 parameter convergence probability, we sampled two individuals per species since calculations do not benefit from
232 adding extra individuals over number of loci (Drummond and Bouckaert 2015). We used VCFtools v.0.1.16 (Danecek
233 et al. 2011) to generate a supermatrix of 12 individuals, including only unlinked biallelic SNPs with 0% missing data
234 as required by SNAPP. The analysis run for 10 million MCMC generations, sampling every 1000 steps, with mutation
235 rate and priors estimated during the chains, and all the other settings set as default. The convergence of the analysis
236 was checked using Tracer v.1.7 (Rambaut et al. 2018) and, as suggested by the software, we discarded the first 10%
237 of trees as burn-in. We analyzed the tree files with SNAPP-TreeSetAnalyser v.2.5.2 to identify species trees that are
238 contained in the 95% highest posterior density (HPD) set and using 10% of topologies as burn-in. Densitree v.2.5.2
239 (Bouckaert 2010) was used to visualize the posterior distributions of topologies as cladograms, hence allowing for a
240 clear depiction of uncertainty in the topology.
241
242 **Morphological and morphometric analyses**
243 Macro and micromorphological observations of coral skeletons were performed using light microscopy and
244 scanning electron microscopy (SEM), respectively. Images of the coralla with a reference scale were taken with a
245 Canon G15 digital camera and through a Leica M205 FA stereo-microscope at fixed magnifications. A collection of
246 skeleton images was obtained for each of the examined specimens and of the type specimens. Measurements were
247 done with the ImageJ Analyse tool (Rueden et al. 2017; https://imagej.nih.gov/ij/) from images at known
248 magnification. Six characters on each of five corallites were measured for each specimen: (v1) maximum calice
249 diameter; (v2) minimum calice diameter; (v3) maximum columella diameter; (v4) minimum columella diameter
250 perpendicular to v3; (v5) distance between the centre of the columella and the centre of the columella of the closest

adjacent corallite; (v6) width of the groove among the corallites. A principal component analysis (PCA) was conducted on averaged measures per specimen for the six variables using the PRIMER v.7.0.13 statistical package (Primer-e).

For SEM imaging, fragments of coral specimens were ground, mounted on stubs using silver glue and sputter coated with gold, and examined with a Vega Tescan Scanning Electron Microscope at the SEM Laboratory (UNIMIB). Imaging was conducted to describe and illustrate the following skeletal features of each species for comparative purposes: radial elements relative thickness, height and ornamentation (margin and sides), septal fusion pattern among cycles and with the columella, structure and shape of the columella.

For a glossary of skeletal terms, we followed Budd et al. (2012) and Huang et al. (2014).

Geographic distribution analyses

Occurrence data plotted to obtain species distribution maps came from two different sources: (a) material collected and analyzed from a genomic and morphological point of view for this study (Data S1); (b) specimens with reliable sampling locality information deposited in museum collections housed at the MNHN, National Museum of Natural History, Smithsonian Institution (NMNH, USA), Natural History Musem, London (NHM, the U.K.), the Museum für Naturkunde, Berlin (ZMB, Germany), and the Museum of Tropical Queensland, Townsville (MTQ, Australia) (Taxonomic Account and Data S2). The reliability and objectivity of the latter source were based on the diagnostic morphological characters that we summarized in the nomenclature acts.

To ease the visual identification of large scale biogeographical patterns, and particularly the degree of overlap in species distributions, we used species occurrences to derive geographical ranges for the six coral species using the α-hull procedure (García-Roselló et al. 2015). To select a proper value for the α parameter (that is, ensuring a conservative estimation of species ranges), we started with a very small α (0.001), and then we incremented it progressively in small amounts (0.005), and then largest α value for which all occurrences where included in the resulting range.

Results

The *Leptastrea* colonies sampled for this study belong to five morpho-species currently considered valid (Hoeksema and Cairns 2019), namely the genus type species *L. purpurea* (n=29) (Fig. 1a-d, Fig. S1_1), *L. pruinosa* (n=3) (Fig. 1e-h), *L. transversa* (19) (Fig. 1i-l, Fig. S1_2), *L. bottae* (n=6) (Fig. 1m-p, Fig. S1_3), and *L. inaequalis*

279 (n=9) (Fig. 1q-t, Fig. S1_4). Plocoid specimens with barrel-shaped corallites and distinctive coenosteum grooves from
280 New Caledonia and Papua New Guinea match the east Australian material identified as *L.* cf *bottae* (n=5) by Veron
281 et al. (1977: Figs 300-302) (Fig. 2, Fig. S1_5). A distinctly plocoid morph of *Leptastrea* collected from Mayotte Island
282 and north Madagascar (n=6) does not match any of the existing species descriptions (Fig. 3, Fig. S1_6). Hereafter, we
283 use the name *L. gibbosa* sp. n. for the specimens preliminary identified as *L.* cf *bottae sensu* Veron et al. (1977), and
284 *L. magaloni* sp. n. for the distinct undescribed morph of *Leptastrea* collected from Madagascar and Mayotte. Both
285 names are formally assigned based on genomic, morphological, and distributional evidence in the taxonomic section
286 further in this paper. However, for the sake of clarity, they are used throughout the manuscript in order to avoid
287 nomenclatural confusion.
288
289 **ezRAD phylogenomic inference**
290 The unfiltered holobiont dataset included a total of 8,323 contigs while the coral transcriptome itself had 101,322
291 contigs (= loci). Therefore, the chance of reads mapping and SNP detection was high in the binned case. At the end
292 of the dDocent and rad_haplotyper pipeline, the "holobiont-max" supermatrix included 3,701 loci and a total of 44,162
293 SNPs, the "coral-max" supermatrix 9,573 loci and 62,728 SNPs, the "holobiont-min" supermatrix 2,075 loci and 2,141
294 SNPs, and the "coral-min" supermatrix 2,366 loci and 2,479 SNPs (all alignment data are available upon request to
295 the corresponding author).
296 The phylogenetic trees inferred from the concatenated "holobiont-max" and "coral-max" matrices provided a fully
297 resolved phylogeny of *Leptastrea* species (Fig. 4). They recovered the presence of six strongly supported clades,
298 namely clade I (*L. gibbosa* sp. n.), clade II (*L. purpurea* and *L. pruinosa*), clade III (*L. transversa*), clade IV (*L.*
299 *magaloni* sp. n.), clade V (*L. inaequalis*), and clade VI (*L. bottae*). *Leptastrea gibbosa* sp. n. and *L. magaloni* sp. n.
300 were reciprocally monophyletic with high support values in all analyses. Moreover, *L. gibbosa* sp. n., previously
301 identified as *L.* cf *bottae* (Veron et al. 1977) or *L. bottae* (Veron 2000) based on the traditional morphology-based
302 taxonomy, was clearly separated and distinct from the Indian representatives of *L. bottae*. The three samples matching
303 the typical morphology of *L. pruinosa* from the Gambier Islands (French Polynesia) and New Caledonia were mixed
304 with the many analyzed samples of *L. purpurea* from the Indo-Pacific, without any genomic distinction. The sister
305 relationships between *L. bottae* and *L. inaequalis*, and between the lineage they constitute and *L. magaloni* sp. n. were
306 found in both the phylogenetic trees with strong support values (Fig. 4). Notably, the topologies of the two phylogeny

307 reconstructions were different because of the position of *L. gibbosa* sp. n., which was sister to *L. transversa* in the
308 holobiont tree and sister to the lineage leading to *L. magaloni* sp. n., *L. bottae*, and *L. inaequalis* in the coral tree (Fig.
309 4).

310 The phylogenetic trees inferred from the concatenated "holobiont-min" and "coral-min" datasets (Fig. S2) were
311 much less resolved, presenting low/very low bootstrap support compared to the ones obtained with more loci and
312 more missing data. Nevertheless, the two phylogenetic analyses resolved, with generally low support values, four out
313 of the six molecular clades found based on "holobiont-max" and "coral-max" matrices, including clade I (*L. gibbosa*
314 sp. n.), clade II (*L. purpurea* and *L. pruinosa*), clade III (*L. transversa*), and clade IV (*L. magaloni* sp. n.). Conversely,
315 representatives of the two closely related clades clade V (*L. inaequalis*) and clade VI (*L. bottae*) were mixed.
316
317 **Nearly complete mitogenome and rDNA phylogenetic inference**
318 Mapping reads to the mitochondrial reference genome of *Polycyathus chaishanensis* resulted in a mean of 2,539
319 reads, covering 91% of the reference sequence per library (Data S1). The mitogenome alignment was 10,837 bp long
320 and revealed low divergence across samples, with 98% of the positions conserved, and only 214 variable sites of
321 which 165 were parsimony-informative (Data S3). By excluding the two outgroup sequences, the alignment contained
322 140 variable positions of which 99 were parsimony-informative. Concerning the rDNA arrays, approximately 17,269
323 reads mapped to the rDNA reference sequences, with a mean of 83% of the reference sequence covered (Data S1).
324 The rDNA multiple alignment consisted of 5,835 bp and displayed low genetic variability across the samples, being
325 conserved for 98.9% nucleotide positions, with a total of 66 variable bp of which 53 were parsimony-informative
326 (Data S4). Considering only the ingroup, the variable positions decreased to 43 of which 38 were parsimony-
327 informative.

328 The phylogeny reconstructions based on mitogenomes and rDNA resolved clade I (*L. gibbosa* sp. n.), clade II (*L.*
329 *purpurea* and *L. pruinosa*), clade III (*L. transversa*), and clade IV (*L. magaloni* sp. n.) (Fig. 5), although with weaker
330 support values than the ones obtained from the phylogenetic trees inferred based on the holobiont and coral ezRAD
331 data. Both mitogenomes and rDNA trees failed to recover clade V (*L. inaequalis*) and clade VI (*L. bottae*) as distinct
332 lineages as samples of these two species grouped together in a single clade without genetic distinction. Both
333 phylogenetic analyses placed *L. magaloni* sp. n. and the lineage including *L. inaequalis* and *L. bottae* as sister taxa, in
334 agreement with the holobiont and coral ezRAD topologies. Moreover, *L. transversa* and clade II (*L. purpurea* and *L.*

335 *pruinosa*) had a sister relationship in both trees. Similarly to the discordance described between the holobiont and
336 coral ezRAD trees, the mitogenome and rDNA tree topologies differed in the placement of *L. gibbosa* sp. n. which
337 was the basal species of *Leptastrea* according to the mitogenome whereas it was the sister taxon of the lineage leading
338 to *L. transversa* and the clade with *L. purpurea* and *L. pruinosa.*

339 The phylogenetic trees based on the barcoding loci COI and ITS were mostly unresolved, generally displaying
340 very low bootstrap support (Fig. S3). In particular, the phylogeny reconstruction inferred from COI resolved clade II
341 (*L. purpurea* and *L. pruinosa*) with high support value (100) and clade I (*L. gibbosa* sp. n.) without any significant
342 support values. All the samples from the remaining four clades identified by the ezRAD phylogenies were mixed and
343 their relationships unresolved. The phylogenetic hypothesis based on ITS resolved clade II (*L. purpurea* and *L.*
344 *pruinosa*) with medium support value (80) and clade I (*L. gibbosa* sp. n.) with low support value (56). Clade II (*L.*
345 *transversa*) was not monophyletic but its samples did not group with any other species. Samples of clade IV, V, and
346 VI clustered together without any genetic structuring.
347
348 **Species delimitation analyses**
349 We tested eight species delimitation models with the BFD* method to identify the number of lineages in *Leptastrea*
350 (Table 1). The best-supported model involved considering the six molecular clades (from I to VI) found in the ezRAD
351 phylogenies as six distinct species (model 5, MLE = -12,650.36, BF = -). The other seven models were ranked as
352 follows: proposed EzRAD phylogenies but splitting *L. purpurea* and *L. pruinosa* (model 6, MLE = -12,659.39, BF=
353 18.06), proposed mitogenome and rDNA phylogenies (model 8, MLE = -12,680.83, BF= 60.94), current taxonomy
354 (model 2, MLE = -13,128.18, BF= 955.64), proposed EzRAD phylogenies but lumping *L. purpurea* with *L pruinosa*
355 and *L. transversa* (model 7, MLE = -13,561.36, BF= 1,822), current taxonomy but lumping *L. purpurea* with *L.*
356 *pruinosa* and *L. transversa* (model 4, MLE = -14,010.44, BF= 2,720.16), current taxonomy but lumping *L. purpurea*
357 with *L. transversa* (model 3, MLE = -14,015.65, BF= 2,730.58), one single species (model 1, MLE = -15,329.96, BF=
358 5,359.2). In summary, BFD* supported the findings of the two phylogeny reconstructions presented in Fig. 4.

359 The species tree was estimated based on 1,857 unlinked biallelic coral SNPs with 0% missing data (Fig. 6a). We
360 followed the best-supported model from the BFD* analysis, *i.e.* considering the six molecular clades (from I to VI)
361 found in the concatenation-based ezRAD phylogenies as six distinct species. Following the SNAPP- TreeSetAnalyser
362 package, only one topology summarized the 95% HPD consensus tree. This was consistent with the topology of the

363 concatenation-based tree inferred from the "holobiont-max" supermatrix. Two major groups, each of which was
364 composed by three species, were resolved: the first clade recovered the sister relationship between *L. bottae* and *L.*
365 *inaequalis*, which were sister to *L. magaloni* sp. n.; the second group supported the sister relationship between *L.*
366 *transversa* and *L. gibbosa* sp. n., which were sister to *L. purpurea*. All the nodes received full support values with a
367 Bayesian posterior probability of 1, except the one referring to *L. bottae* and *L. inaequalis*, supported by 0.99.
368
369 **Morphometric analyses**
370 A total of 74 *Leptastrea* colonies, including type specimens, were included in our morphometric analyses based
371 on six variables (v1-v6) measured on each (5 replicates per variable). Mean values (st. dev.) and the number of colonies
372 per species are provided in Data S5. Multivariate analysis of the skeletal variables per specimen dataset could separate
373 specimens into five groups (Fig. 7) corresponding to *L. transversa*, *L. bottae*, *L. inaequalis*, *L. gibbosa* sp. n. and *L.*
374 *magaloni* sp. n., thus matching the groupings obtained by genomic analyses. However, specimens of the
375 morphologically variable *L. purpurea* (Fig. S4a-h) completely overlapped with *L. magaloni* sp. n. and partially with
376 *L. bottae* along the first two PC of the PCA plot (Fig 7). The strongest correlations were between PC1 and the linear
377 distance among centres of adjacent corallites (v5, r = 0.66) and the maximum calice diameter (v1, r = 0.63). Similarly,
378 moderate positive correlations were recovered between initial variables and PC2, the stronger being with v4 (minimum
379 columella diameter, r = 0.62) and v5 (r = 0.59). Gap width among corallites was observed and measured exclusively
380 in specimens of *L. gibbosa* sp. n. and *L. inaequalis*. Despite the former having consistently smaller corallite and
381 columella features than the latter (Data S5), the gaps width was similar in the two species.
382
383 **Geographic distribution analyses**
384 The newly obtained distribution maps of the six *Leptastrea* species are illustrated in Fig. 6b. *Leptastrea purpurea*
385 and *L. bottae* exhibit a widespread and overlapping geographic distribution in the Indo-Pacific. Notably, the total
386 number of occurrences for these two species considerably increased based on the information obtained from museum
387 collections and the taxonomic literature. *Leptastrea gibbosa* sp. n. is distributed across Papua New Guinea, Australia,
388 and New Caledonia. The remaining three species, *i.e. L. bottae*, *L. inaequalis*, and *L. magaloni* sp. n., display an Indian
389 Ocean distribution with some distinctions. *Leptastrea bottae* appears to have a disjoint distribution, occurring in the
390 seas around the Arabian Peninsula (Red Sea and the Gulf of Aden) and in the eastern Indian Ocean (Cocos Islands).

391 *Leptastrea inaequalis* is found in the seas around the Arabian Peninsula and in the western-central Indian Ocean
392 (Mayotte Island, Seychelles, Maldives, and Laccadive Sea). *Leptastrea magaloni* sp. n. is restricted to the southern-
393 western Indian Ocean (Mayotte Islands, Madagascar, and South Africa).
394
395 **Taxonomic Account**
396 Based on the results arising from genomic, morphological, and distributional data, we propose a revised taxonomy
397 for the examined *Leptastrea* species. In particular, (a) *L. gibbosa* sp. n. and *L. magaloni* sp. n. are formally described;
398 (b) *L. pruinosa* is considered a junior synonym of *L. purpurea*; (c) *L. bottae* and *L. inaequalis* geographic distributions
399 are revised and they are now considered restricted to the Red Sea and Indian Ocean (Data S2).
400
401 Order Scleractinia Bourne, 1900
402 Family *Incertae Sedis*
403 Genus *Leptastrea* Milne Edwards and Haime, 1849
404 **Synonyms:** *Bathyastrea* Milne Edwards and Haime, 1849, *Orbicella* (*Leptastraea*) Milne Edwards and Haime, 1849,
405 *Orbicella* (*Leptastrea*) Milne Edwards and Haime, 1849.
406 **Type species:** *Leptastrea roissyana* Milne Edwards and Haime, 1849 (=*Astrea purpurea* Dana, 1846).
407 **Species included:** *Leptastrea aequalis* Veron, 2000, *Leptastrea bewickensis* Veron, Pichon and Best, 1977, *Leptastrea*
408 *bottae* (Milne Edwards and Haime, 1849), *Leptastrea gibbosa* sp. n. Benzoni and Arrigoni, 2019, *Leptastrea*
409 *inaequalis* Klunzinger, 1879, *Leptastrea magaloni* sp. n. Benzoni and Arrigoni, 2019, *Leptastrea purpurea* (Dana,
410 1846), *Leptastrea transversa* Klunzinger, 1879.
411
412 ***Leptastrea gibbosa* sp. n.** Benzoni and Arrigoni, 2020 (Fig. 2, Figs. S1_5, S4m-p)
413 **Synonymy:** *Leptastrea bottae* (Milne Edwards and Haime, 1849), Crossland 1952, Plate I, Fig. 4; Plate II, Fig. 3;
414 *Leptastrea bottai* (Milne Edwards and Haime, 1849) Chevalier, 1975, Plate II, Figs. 8-9; Plate III, Fig. 5; Plate
415 XXXVIII, Figs. 4-5, 11; *Leptastrea* cf *bottae* (Milne Edwards and Haime, 1849), Veron et al. 1977, Figs. 300-302,
416 466; *Leptastrea inaequalis* Nishihira and Veron 1995; Veron 2000, Figs. 3-6 and corallite image.
417 **Etymology:** *Gibbosus*, "humped" in Latin, refers to the uneven aspect of the colony surface caused by the protruding
418 rounded corallites.

Type material: MNHN-IK-2012-9822 Magic Pass, Madang, Papua New Guinea (5°11.356' S; 145°49.637' E), MNHN NIUGINI Expedition, 11/11/2012 (coll. F. Benzoni: UNIMIB PFB082).

Other material examined: Australia: BM 1934.5.14.444 (GBR Expedition: n°407), 1934; MTQ: G68954 Elisabeth and Middleton (coll. J.E.N. Veron); G68956 Yule Reef, Queensland, 02/11/1974 (coll. J.E.N. Veron & M. Pichon); G68955 Middleton Reef, 05/12/1981 (coll. J.E.N. Veron); G36744 Jewell Reef, Queensland (14°23' S; 145°22 'E); G68957 Jewell Reef, Queensland (coll. J.E.N. Veron & M. Pichon); G65509 Elisabeth Reef (29°56' S; 159°4' E), 2007 (coll. A. Noreen); G36748 Lizard Island, Queensland (14°40' S; 145°27' E); G36750 Bowl Reef, Queensland (18°31' S; 147°32' E); G36745 Fantome Island, Palm Islands (18°41' S; 146°31' E); G39298 Bullumbooroo Bay, Great Palm Islands (18°43' S; 146°34' E); G36749 Hook Island, Whitsunday Islands (20°04' S; 148°57' E); G39297 Swain Reefs (21°07' S; 142°46' E); JCU AU519 Mellish Reef, Coral Sea (17°25.591' S; 155° 51.196' E), JCU Coral Sea Cruise, 15/12/2018 (coll. F. Benzoni); **Papua New Guinea** UNMIB PFB805 Kavieng (2°37.224' S; 150° 31.750' E), 22/08/2014 (coll. F. Benzoni). **New Caledonia**: MNHN-IK-2016-10 (coll. J.-P. Chevalier: P152g1); MNHN-IK-2016-9 (coll. J.-P. Chevalier: P152g2); MNHN unregistered Surprise Atoll, d'Entrecasteaux Reefs (coll. J.-P. Chevalier: SU14c); HS0330 Extérieur Grand Récif Tetembia, 02/02/1987 (coll. IRD-plongeur); IRD HS1678 Kouakoué (21°47.842' S; 166°37.661' E), CORALCAL1, 25/03/07 (coll. F. Benzoni & G. Lasne); HS1681 ST1082 (21°47.842' S; 166°37.661' E), CORALCAL1, 25/03/07 (coll. F. Benzoni & G. Lasne); HS1684 Kouakoué, Grande Terre (21°47.842' S; 166°37.661' E), CORALCAL1, 25/03/07 (coll. F. Benzoni & G. Lasne); HS2189 îlot du Mouillage, Chesterfield Islands (19°47.191' S 158°27.519' E) CORALCAL2 19/07/08 (coll. G. Lasne & J. Butscher); HS2344 Belep Island, Great North Lagoon (19°32.182' S 163°34.380' E), CORALCAL3, 15/03/09 (coll. G. Lasne & J. Butscher); HS2460 Cook Reef, Great North Lagoon (19°02.989' S 163°38.857' E), CORALCAL3, 21/03/09 (coll. G. Lasne & J. Butscher); HS3167 Moneo, Grande Terre (21°03.354' S; 165°35.297' E), CORALCAL4; HS3653 Uaté-Oro Bay, Isle of Pines (22°35.2' S; 167°31.73' E), CORALCAL5, 01/10/2015 (coll. F. Benzoni); HS3740 Kuto, Isle of Pines (22°39.101' S; 167°21.154' E), CORALCAL5, 05/10/2015 (coll. F. Benzoni).

Description: Corallum encrusting to submassive (Fig. 2a-c, Fig. S1_5), circular to irregular in outline, rarely exceeding 15 cm in diameter. Budding extracalicular. Corallites can be evenly arranged on the corallum surface or variably exsert and inclined, both arrangements can occur in different parts of the same colony (Fig. S1_5). Among the corallites, 0.4 mm wide (± 0.1 s.d.) grooves and pits alternate with an irregularly developed coenosteum (Fig. 2a-e, g, Fig. S4m-p). Longitudinal sections of the coralla show that this is composed of distinct solid beam-like structures

447 transversally joining adjacent corallite walls all along their length (Fig. 2f; Crossland 1952: Plate II, Fig. 2). These
448 structures have been called verrues (warts, in French) by Chevalier (1975: 56) and beams (Crossland 1952: 116) in
449 descriptions of material we examined and that is here ascribed to *Leptastrea gibbosa* sp. n.. As shown also in the
450 skeleton histological sections by Chevalier (1975: Fig. 26), the beams result from the fusion of processes laterally
451 developing from, and all along, the outer wall of adjacent corallites (Fig. 2f). Calice outline mainly circular, average
452 maximum diameter 1.6 mm (± 0.2 s.d.) and minimum diameter 1.3 mm (± 0.1 s.d.) (Fig. 2g). Corallite outline circular
453 to irregularly polygonal with rounded corners (Fig. 2d-e, g). Two complete and one incomplete cycles of radial
454 elements are present (Fig. 2i). S1 reaches the columella, its septa typically exsert from the colony surface (Fig. 2h)
455 and with a slightly undulating upper margin (Fig. 2l). S2, of variable length, shorter and less exsert than S1. S3
456 incomplete and very reduced (Fig. 2i-j). Septal sides irregularly covered in well-spaced pointed ornamentations (Fig.
457 2l). Beyond the corallite wall, radial elements are clearly distinguishable, tightly packed and finely granulated (Fig.
458 2j). Columella formed by mostly fused trabecular processes and forming granulations at their upper end (Fig. 2i-k),
459 0.6 mm (± 0.1 s.d.) in maximum diameter. A giant corallite can form in some coralla (Fig. 2b, Fig. S4p; Crossland
460 1952: 116, Plate II, Fig. 3; Veron et al 1977: 156, Figs. 301, 158). This is usually twice as large as the others in the
461 same colony and more exert (Fig. S4p). It contains up to 4 complete cycles of septa with both S1 and S2 reaching the
462 columella formed by multiple trabecular processes and fusing with it. These odd oversized corallites do not seem to
463 be linked to an ongoing budding process. In addition to the present description, the reader can also refer to the detail
464 treatment of specimens P152g2 (MNHN-IK-2016-9) and SU14c (MNHN unregistered) in Chevalier (1975: 57-58).
465 Polyps of *Leptastrea gibbosa* sp. n. have a rather consistent brown colouration and their tentacles are usually retracted
466 at daytime (Fig. S1_5). The tissue covering the outer part of the corallites and the coenosteum is yellowish to light
467 green, becoming almost transparent in parts where corallites are more exsert or irregularly arranged (Fig. S1_5f, g).
468 This species was most often encountered on the upper part of the reef slope between 2 and 15 m in well-lit
469 environments.
470 **Molecular phylogeny:** Recovered as a monophyletic lineage (clade I) with high node support values in all
471 phylogenetic trees presented in this study (Figs. 4-5). This species is clearly genomically distinct from *L. inaequalis*
472 (clade V) and *L. bottae* (clade VI). Although the phylogenetic placement of the species is unstable across the
473 phylogenetic analyses, the species tree indicates that the species is sister to *L. transversa* (Fig. 6a).

474 **Remarks:** This species has been referred to as *L. inaequalis*, *L. bottae* and/or *L.* cf *bottae* (Crossland 1952; Veron et
475 al. 1977; Nishihira and Veron 1995; Veron 2000). This confusion likely stems from the fact that both *L. inaequalis*
476 and *L. bottae* share with L. *gibbosa* sp. n. a typically circular calice outline (Figs. 1m-o, q-s). Moreover, the irregular
477 corallite arrangement and formation of grooves and pits described above for *L. gibbosa* sp. n. are also observed in *L.*
478 *inaequalis* (Figs. 1q-s, Fig. S4q-t), and the gaps among corallites have similar dimensions in both species (Data S5).
479 However, *L. gibbosa* sp. n. is distinguished from both *L. inaequalis* and *L. bottae* based on its smaller calice and
480 columella dimensions (Data S5) and the presence of 2 rather than 3 complete cycles of septa. Finally, *L. gibbosa* sp.
481 n. is restricted to the Pacific Ocean whereas *L. inaequalis* and *L. bottae* are largely sympatric and occur in the Red Sea
482 and Indian Ocean (Fig. 6b).
483 **Distribution:** Western and central Pacific Ocean (Papua New Guinea, New Caledonia, Australia). Possibly in Japan
484 although the record in Nishihira and Veron (1995) could not be confirmed because the published image is that of a
485 specimen from Australia already published by Veron et al. (1977: Fig. 301).
486
487 ***Leptastrea magaloni* sp. n.** Benzoni and Arrigoni, 2020 (Fig. 3, Figs. S1_6, S4y-ab)
488 **Etymology:** This species is named after Mme Helene Magalon (Université de La Réunion), chief scientist and
489 organizer of the 2016 MAD Expedition to north Madagascar during which this species previously only collected in
490 Mayotte Island was detected and collected.
491 **Type material:** Holotype MNHN-IK-2012-9823 Bouzi, Mayotte Island (12°48'44.94"S, 45°14'29.16"E), Tara
492 Oceans Expedition, 18/06/2010 (coll. F. Benzoni: UNIMIB MY345).
493 **Other material examined: Madagascar**: MTQ G62190 Nosy Be (13°20'0"S; 48°15'0"E), Jan 2002 (coll. J.E.N.
494 Veron); MNHN-IK-2016-230 (coll. code IRD MD260) west Nosy Be (13°19'28.10"S, 48° 4'37.82"E), 30/10/2016,
495 MAD Expedition (coll. F. Benzoni); IRD, MAD Expedition (coll. F. Benzoni): MD222 Nosy Lava west
496 (14°33'17.29"S, 47°33'59.71"E), 27/10/2016; MD225 Nosy Lava west (14°33'17.29"S, 47°33'59.71"E), 27/10/2016;
497 MD266 Nosy Sakatia (13°19'1.67"S, 48° 8'49.88"E), 30/10/2016; MD274 Nosy Sakatia (13°19'1.67"S, 48°
498 8'49.88"E), 30/10/2016; **South Africa**: BMNH 1961.7.18.3-5 Inyoni, 1948 (coll. T.A. Stephenson).
499 **Description:** Corallum encrusting to massive (Fig. 3a-c, Fig. S1_6), circular to irregular in outline, the largest colony
500 observed 20 cm in diameter. Budding predominantly extracalicular (Fig. 3b, g), occasionally intracalicular (Fig. 3d).
501 Corallites plocoid, variably exsert but not inclined on the corallum surface (Fig. S1_6a-e). Coenosteum present,

compact, and variably developed (Fig. 3a-h). Calice outline mainly circular to elliptical (Fig. 3a-d, g), irregular with rounded corners in some specimens (Fig. 3e-f, h-i). Calice average maximum diameter 4.7 mm (± 0.7 s.d.) and minimum diameter 3.9 mm (± 0.6 s.d.) (Data S5). Four complete cycles of radial elements are present (Fig. 3h-i, k), a fifth incomplete one can be observed in larger corallites (Fig. S4y). S1 and S2 equal or sub-equal, septa of higher cycles increasingly thinner and shorter (Fig. 3k). S1 and S2 upper septal margin slightly arched (Fig. 3i, l). S1-2 reach the columella, S3 and S4 free (Fig. 3g-h) or fused with S2 and S3, respectively (Fig. 3e-f, Fig. S4y, aa-ab). S1-3 bear at their proximal end a granular palar structure of the same size and shape as the columellar processes. The inner upper margin of S3 forms obvious paddle-shaped structures (white arrows in Fig. 3k). S4 devoid palar structures (Fig. 3k). Septal sides densely covered in obvious granules (Fig. 3j-l). Beyond the corallite wall, radial elements form granulated costae which continue over the coenosteum (Fig. 3j). Columella composed of granules (Fig. 3h-i), 1.1 mm (± 0.1 s.d.) in maximum diameter, and 0.8 mm (± 0.1 s.d.) in minimum diameter.

Polyps of *Leptastrea magaloni* sp. n. are mostly typically fully extended at daytime (Fig. S1_6a-c, f-g), with green or brown tentacles, and a distinctive white oral disc (Fig. S1_6). The tissue among the polyps is beige to brown (Fig. S1_6f, g). This species was encountered between 15 and 25 m in turbid and protected environments, often growing on hard substrate partially or completely covered in terrigenous sediment.

Molecular phylogeny: Recovered as a monophyletic lineage (clade IV) with high node support values in all phylogenetic trees presented in this study (Figs. 4-5). This species is sister to the lineage leading to *L. bottae* and *L. inaequalis* (Fig. 6a). The three species thus belong to a lineage which appears to be restricted to the Red Sea and Indian Ocean regions.

Remarks: Among its congeners, *Leptastrea magaloni* sp. n. is similar to, yet distinct from, *L. purpurea* and *L. aequalis*. Within the wide range of *L. purpurea* morphological variability (Fig. S4a-h), *L. magaloni* sp. n. most closely resembles specimens displaying the *L. pruinosa* morphology (Figs. 1e-h), a species here synonymised with *L. purpurea*. However, although average calice and columella diameter are similar in *L. magaloni* sp. n. and *L. purpurea*, the two species can readily be told apart: the former has distinctly plocoid, typically protruding, more rounded and uniformly sized corallites, while the latter is characterised by cerioid to sub-cerioid, polygonal and variably sized corallites within the same corallum (Fig. S4a-h). Furthermore, *L. magaloni* sp. n. polyps are usually fully extended at daytime, a condition seldom observed in the field for *L. purpurea* (Fig. S1_1a-e, g). However, when tentacles of *L. purpurea* are fully extended (Fig. S1_1f), they are shorter, thinner, and less crowded than those of *L. magaloni* sp. n.

530 (Fig. S1_6f-g). *Leptastrea aequalis*, originally described from from Cocos (Keeling) Atoll, shares with *L. magaloni*
531 sp. n. a similar plocoid to sub-plocoid arrangement, a rounded calice outline, and protruding corallites. Based on the
532 holotype (WAM Z12912) illustrations and the original description (Veron 2002: Figs. 306-307), and the specimens
533 housed at MTQ identified as *L. aequalis* by JEN Veron, differences with *L. magaloni* sp. n. are clear. Corallite and
534 columella size are larger in *L. magaloni* sp. n. (4.0-5.4 mm) than in *L. aequalis* (2.5-3.5 mm) (Veron 2002). Moreover,
535 in the latter species "there are no paliform lobes" (Veron 2002: 168), while palar structures are variably but
536 consistently developed in the former species. Finally, in *L. aequalis* corallites are often uniformly inclined on the
537 colony surface, while in *L. magaloni* sp. n. they can be variably exsert from the coenosteum but not inclined.
538 **Distribution:** Southern and western Indian Ocean (SWIO). Currently reported from Mayotte Island, north
539 Madagascar, and South Africa.
540
541 ***Leptastrea purpurea*** (Dana, 1846)
542 (Figs. 1a-h, S1_1, S4a-h)
543 *Astraea (Fissicella) purpurea* Dana, 1846.
544 *Leptastrea purpurea* (Dana, 1846) Crossland, 1952, Pl. I, Fig. 5, Pl. III, Fig. 3; Chevalier 1975, Pl. II, Fig. 3-4, Pl. III,
545 Fig. 2; Veron et al. 1977, Figs. 303-310, 467; Wijsman Best 1980, Pl. 3, Figs. 1-2; Scheer and Pillai 1983, Pl. 31, Figs.
546 11-12; Sheppard and Sheppard 1991, Fig. 159; Veron 2000, Figs. 1, 3-5; Claereboudt 2006 and figures therein; Dai
547 and Horng 2009 and figures therein; Al Tawaha et al. 2019, Figs. 1-4.
548 *Leptastrea pruinosa* Crossland, 1952 Crossland, 1952, Pl. III, Fig. 1; Veron et al 1977, Figs. 319-321, 323-324, 326;
549 Wijsman Best 1980, Pl. 2, Fig. 1; Veron 2000, Fig 8; Claereboudt 2006 and figures therein; Dai and Horng 2009 and
550 figures therein; Pichon et al. 2010, Figs. 1, 4.
551 *Leptastrea* cf *pruinosa* Crossland, 1952 Chevalier 1975, Pl. II, Fig. 5, Pl. III, Fig. 7.
552 *Leptastrea transversa* Klunzinger, 1879 Chevalier 1975, Pl. II, Fig. 7; Veron et al 1977, Figs. 314-316, 468; Veron
553 2000, Figs. 4, 6.
554 **Holotype:** USNM 75, Fiji, U.S. Exploring Expedition.
555 **Other material examined:** complete list in Data S2.
556 **Remarks:** Both genomic and morphological data clearly indicate that the distinction between *L. purpurea* and *L.*
557 *pruinosa* is unnecessary and, therefore, the latter species is formally considered a junior synonym of the former taxon.

From a genomic point of view, the two species are mixed within a single lineage (clade II) in the phylogenetic trees based on both the holobiont and the coral datasets (Fig. 4) and no genomic distinction between them is found. This is a robust result considering that the two datasets include a total of 3,701 and 9,573 loci, respectively. The phylogenomic analyses are further confirmed by the species delimitation analysis BFD* (Table 1), where the best-supported model is the one considering *L. purpurea* and *L. pruinosa* as a single species (model 5, MLE = -12,650.36, BF = -), in constrast to the scenario where the two species are considered as distinct taxa (model 6, MLE = -12,659.39, BF= 18.06). From a morphological point of view, there are differences between the holotypes of the two species (Fig. 1) mainly in terms of corallite arrangement (i.e more ceriod in *L. purpurea* and plocoid in *L. pruinosa*). However, the study of a large collection of specimens allowed us to verify that these two typical morphologies fall within the range of variation of the same species. Thus, concordant genomic and morphologic evidence support the synonymy.

Identification key to the species examined in this study

1a Adjacent corallite walls not fused and distinct	2
1b Adjacent corallite walls fused or touching	4
2a Calice outline mostly circular	3
2b Calice outline polygonal or irregular	4
3a Grooves among adjacent corallites present	5
3b Grooves among adjacent corallites absent	6
4a Columella lamellar or composed of 2-4 aligned granules	*L. transversa*
4b Columella circular to elliptical and composed of >4 granules	*L. purpurea*
5a Three complete cycles of septa	*L. inaequalis*
5b Two complete cycles of septa (third incomplete or absent)	*L. gibbosa* sp. n.
6a Three complete cycles of septa	*L. bottae*
6b Four complete cycles of septa	*L. magaloni* sp. n.

Discussion

In this study we evaluated species boundaries within a scleractinian coral genus sampled across the Indo-Pacific by integrating genomics, morphology, and biogeography. The combination of methods allowed us to delimit six

586 species in *Leptastrea*, two of which new to science, and to update their geographic distribution. All species were fully
587 resolved in the phylogenomic framework based on ezRAD data and could be distinguished based on revised diagnostic
588 morphological characters as shown in the proposed identification key. The novel aspects of this study are: the
589 widespread sampling spanning the entire Indo-Pacific, the unprecedented phylogenetic resolution obtained from the
590 ezRAD method, and the integration of different lines of evidence for species delimitation and ultimately in a
591 taxonomic revision.

592 We are now able to answer the three questions raised in the introduction: (a) closely related and morphologically
593 similar coral species can be distinguished by analyzing large collection of specimens spanning nearly complete
594 geographic ranges of species under the integration of reduced-genome data (and not a set of barcoding genes) with
595 detailed morphometric analyses; (b) once a robust species delimitation framework is obtained (a), we can look at
596 diagnostic morphological characters among the large collection of specimens, unambiguously telling apart
597 intraspecific and interspecific morphological variation, as we presented with the identification key; (c) once diagnostic
598 skeletal structures are found for species (b), we can better understand the species distribution ranges by correctly
599 identifying specimens deposited at museum collections and/or illustrated in reference literature.
600
601 **Improving phylogeny and species delimitation resolution in corals**

602 Our phylogenetic and species delimitation analyses based on ezRAD data provided a robust and fully resolved
603 hypothesis of the examined *Leptastrea* across the tropical Indo-Pacific. The results from all genomic analyses
604 consistently resolved six species, partially rejecting the current taxonomy of seven species ascribed to the genus (Figs.
605 4 and 6, Table 1). The phylogenetic resolution we obtained from both the holobiont and coral ezRAD datasets is
606 unprecedented. Such resolution is even more remarkable when compared to the results obtained from the two
607 traditional barcoding loci COI and ITS (Fig. S3) and from the nearly complete mitogenomes and rDNA arrays (Fig.
608 5). In fact, COI and ITS supported the separation of only two out of the six species, *i.e. L. gibbosa* sp n. and *L.*
609 *purpurea*, whereas *L. magaloni* sp. n., *L. bottae*, and *L. inaequalis* were consistently grouped in an unresolved
610 polytomy. Considering the nearly complete mitogenome and rDNA sequences improved the overall tree resolution.
611 However, the trees obtained from these datasets still persistently failed to separate *L. bottae* from *L. inaequalis*, two
612 admittedly morphologically similar but distinct species (Fig. 1, Fig. S4q-x). The comparison among these different
613 genetic datasets in *Leptastrea* may lead to a re-evaluation of the published molecular phylogenies and species

614 delimitation attempts in corals based on single or few barcoding genes (Kitahara et al 2016). Although the
615 mitochondrial genome of Anthozoa and Porifera evolves slower than the one of the other Metazoa (Shearer et al.
616 2002; Hellberg 2006), several mitochondrial regions have been frequently used to infer phylogenetic relationships
617 among corals (Kitahara et al. 2016). Based on our results, although the application of single barcodes represents a
618 useful strategy for rapid coral species assessments, the results obtained from mitochondrial and rDNA regions should
619 be cautioned for species level resolution because of their low substitution rates.

620 In our study, the phylogenetic analyses inferred with more loci, and thus more missing data, were better resolved
621 at both deep and shallow nodes than the ones based on less loci and low percentage of missing data (Fig. 4, Fig. S2).
622 Notably, the phylogeny reconstructions obtained with about 2,000 loci from both coral and holobiont datasets without
623 any missing data failed to distinguish *L. bottae* and *L. inaequalis*. Nevertheless, although the presence of six species
624 was consistently detected with very strong support values, we observed notable differences in gene tree topologies
625 between the concatenation-based "holobiont-max" and "coral-max" phylogenies, in particular the position of *L.*
626 *gibbosa* sp. n. (Fig. 4). Moreover, the fully-supported topology of the species tree inferred from unlinked biallelic
627 coral SNPs without missing data (Fig. 6a) was identical to the one of the gene tree based on the "holobiont-max"
628 dataset (Fig. 3a). Differences in topologies inferred from RADseq data have been already documented in several cases
629 (Hou et al. 2015; Massatti et al. 2016; Suchan et al. 2017; Rancilhac et al. 2019). In our case, several factors may be
630 hypothesized to explain this discordance: (a) the holobiont tree is poorly supported at several nodes and especially the
631 phylogenetic position of *L. gibbosa* sp. n. is not resolved under the ML criterion; (b) difficulties in resolving
632 interspecific relationships may be associated with incongruences in the phylogenetic signals associated with different
633 sets of loci from the holobiont and coral supermatrices (Gori et al. 2016); (c) the different filtering options yielding to
634 various levels of missing data may have generated different tree topologies (Wagner et al. 2013; Eaton and Ree 2013);
635 (d) concatenating sequence data from thousands of loci does not account for the individual history of these loci
636 (Sanderson et al. 2003), and, since gene histories differ from species histories, concatenation approaches in some cases
637 do not produce accurate species trees (Kubatko and Degnan 2007); (e) the proportion of missing data increases with
638 interspecific evolutionary distances as a consequence of the loss of the restriction sites (Gautier et al. 2013; Cariou et
639 al. 2013); (f) in case of rapid and recent radiations, gene trees may depict different evolutionary histories due to
640 incomplete lineage sorting (Avise et al. 2008) and RADseq datset may be useful for resolving species boundaries but
641 more research is needed to develop best practices for defining interspecific relationships. Unfortunately, in our case

642 we cannot provide any age estimates of the analyzed species due to lack of fossil calibration. Indeed, we retrieved
643 images of the few occurrences supposed to belong to extinct *Leptastrea* species (Paleobiology Database,
644 https://paleobiodb.org/) but the morphology of these specimens could not be unequivocally associated to this genus.
645 Incongruence between traditional morphology- and molecular-based species identification is common in
646 scleractinian corals and corals more broadly (Kitahara et al. 2016; McFadden et al. 2017). Although cryptic species
647 have been documented in several coral genera (Flot et al. 2011; Stefani et al. 2011; Pinzón et al. 2013; Warner et al.
648 2015; Richards et al. 2016; Arrigoni et al. 2019), the discordance between morphology and genetics based on
649 barcoding genes is frequently caused by methodological problems associated with both datasets. It is often challenging
650 to separate intraspecific and interspecific morphological variation, and several skeletal structures are affected by
651 convergence, stasis, and homoplasy (Fukami et al. 2008; Paz-García et al. 2015). This has caused uncertainties and
652 led to the description of morphospecies not representing the actual outcome of an evolutionary process. Additional
653 identification problems and incorrect synonymies have stemmed from a lack of consideration for the actual type
654 material morphology. In fact, coral morphospecies thought to be widespread in the Indo-Pacific have recently been
655 shown to be comprised of multiple, often geographically distinct, lineages (Forsman et al. 2009; Schmidt-Roach et al.
656 2014). This is the case of *L. bottae* and *L. inaequalis*, historically confused (Veron 2000) or synonymised (Chevalier
657 1975; Veron et al. 1977; Wijsman-Best 1980; Scheer and Pillai 1983; Sheppard and Sheppard 1991) (Data S2) and
658 considered widespread (Veron 2000) due to identification evidently not based on type material examination. Our
659 results showed that the two species are actually distinct and restricted to the Red Sea and Indian Ocean where they are
660 sympatric (Al Tawaha et al. 2019; Berumen et al. 2019), while their records from the Pacific (Crossland 1952;
661 Chevalier 1975; Veron et al. 1977; Veron 2000) were based on material here formally described as *L. gibbosa* sp. n.,
662 a genetically (Figs. 4-6a) and morphologically (Fig 7, Data S5) distinct species. In other cases, such as in that of *L.*
663 *purpurea* and *L. pruinosa*, two or more nominal species were shown to be different names used to refer to a single
664 morphologically variable species (Forsman et al. 2010; Carlon et al. 2011; Paz-García et al. 2015; Arrigoni et al.
665 2016b). Nevertheless, unresolved molecular phylogenies or species complexes may also derive from insufficient
666 genetic variation and lack of phylogenetic resolution of barcoding genes (Frade et al. 2010; Prada et al. 2014; Arrigoni
667 et al. 2016a; Terraneo et al. 2016). The advent of reduced-genome techniques such as RADseq significantly overcome
668 the limitations ofwork based on barcoding loci (Andrews et al. 2016). For example, RADseq approach fully-resolved
669 species boundaries within the common scleractinian *Pocillopora* (Johnston et al. 2017), and the speciose octocorals

Chrysogorgia (Pante et al. 2015), *Paragorgia* (Herrera and Shank 2016), and *Sinularia* (Quattrini et al. 2019). For all these taxa, traditional molecular markers have proved uninformative and previously generated unresolved phylogenies. Therefore, RADseq may opened a new era for coral systematics and phylogeny. This approach produces robust species delimitation hypotheses that may be confronted with the outcome from other lines of evidence such as morphology and biogeography with the final objective of a solid taxonomic framework for scleractinian corals.

Leptastrea *taxonomy*

The bewildering geographical morphological variation of *Leptastrea*, and of*L. purpurea* in particular, is well-documented in the literature (Matthai 1914; Chevalier 1975; Veron et al. 1977; Wijsman-Best 1980; Scheer and Pillai 1983) and has led several authors to confuse this species with other congeners, and especially with the equally common and widespread *L. transversa*. For example, Wijsman-Best (1980), referring to *L. purpurea, L. transversa,* and *L. bottae*, stated "in these the geographical variation extends beyond the interpopulational variation and therefore they may be regarded as dynamically evolving species". Indeed, our morphometric analyses confirmed the skeleton variability of the examined species, and of *L. purpurea* in particular. However, the present study demonstrated that this statement is incorrect because the three species are actually clearly genetically and morphologically distinct, with *L. bottae* also being distinct from the valid *L. inaequalis*, as already discussed in the previous paragraph.

Based on our measurements, *L. purpurea* could not be distinguished from material matching the *L. pruinosa* type morphology and *L. magaloni* sp. n. (Figs. 1 and 7, Data S5). However, while our genomic results showed that the typical *L. purpurea* and *L. pruinosa* morphotypes belong to the same species, and thus led us to consider the latter a junior synonym of the former (Data S2), they also provided evidence that *L. magaloni* sp. n. belongs to a separate lineage from *L. purpurea*. Indeed, although the variables we measured did not allow us to separate *L. purpurea* from *L. magaloni* sp. n. specimens, the latter has a distinctively plocoid corallite arrangement, a more regular septal plan and, overall, a smaller variability of corallite and columella dimensions (Data S5). Moreover, differences in polyp morphology *in vivo* were illustrated for the two species (Fig. S1_1 and S1_6) and highlighted. Specimens of *L. transversa,* including the species holotype (Fig. 1i), albeit similar in corallite shape and arrangement to the *L. purpurea* ones with smaller calice dimensions, were readily distinguished based on the typically thinner columella composed of a series of aligned granules, often fused to form a dash shaped structure (Figs. 1j-l) with which S1 and S2 fuse. Hence, despite considerable confusion between the two species in the published literature (Data S1), they are actually readily

698 distinct upon visual examination of the columella. Phylogenetic and species delimitation analyses based on genomic
699 data confirmed the morphometric findings showing that the former two species were reciprocally monophyletic even
700 with the inclusion of samples collected from very distant or remote localities, such as the Red Sea and French
701 Polynesia.

702 *Leptastrea gibbosa* sp. n., identified as *L. bottae* or *L.* cf *bottae* so far (Veron et al. 1977; Veron 2000), is, among
703 the examined species, the species with the smallest corallite features and, despite similarities with *L. bottae* and *L.*
704 *inaequalis* in corallite shape and arrangement, is readily distinct from both species. The biogeographic implications
705 of this finding are discussed in the next section.

706 Two *Leptastrea* nominal species currently considered valid were not included in our analyses, namely *L. aequalis*
707 and *L. bewickensis*. Nevertheless, we examined the species holotypes and specimens housed at the MTQ and both
708 species appear to be at least morphologically distinct and are here considered valid. Differences between the distinct
709 *L. aequalis* and *L. magaloni* sp. n. are discussed in detail in the Taxonomic Account. *Leptastrea bewickensis* remains
710 a more enigmatic species and its relationships with the morphologically similar *L. purpurea* and the rest of the species
711 in the genus need to be ascertained. Finally, based on the morphological examination of specimens of *Cyphastrea*
712 *agassizi* (Vaughan, 1907) housed at the MTQ, the current species assignation is doubtful and further studies on freshly
713 collected material are needed to verify if the species original assignation to the genus *Leptastrea* was, in fact, correct.
714 Finally, it is important to mention that another benefit of ezRAD is that many markers like SNPs and nearly complete
715 mitogenomes should be compatible and comparable among studies. Therfore, it will be easy to phylogenetically
716 include and compare *L. bewickensis* and *C. agassizi* within our genomic and genetic analyses.
717
718 **Leptastrea *biogeography***

719 It is well-known and documented that the coral maximum biodiversity is located in an area of the Indo-Malay
720 Archipelago known as the Coral Triangle (Hoeksema 2007). The high number of species living in the Coral Triangle
721 seems to be largely due to range expansion into this area of taxa that have evolved elsewhere, thus the region is
722 considered as a center of accumulation of marine biodiversity (Huang et al. 2018). A growing number of studies aimed
723 to evaluate scleractinian species boundaries found unexpected biogeographic patterns and several lineages restricted
724 to the Indian Ocean (for a review see Kitahara et al. 2016). Genetic data revealed several cases of evolutionary breaks
725 between Indian and Pacific coral populations traditionally identified as the same widespread Indo-Pacific species, and

726 that these *de facto* are included multiple distinct species with allopatric and geographically circumscribed distributions
727 (Flot et al. 2011; Stefani et al. 2011; Arrigoni et al. 2012; Pinzón et al. 2013; Kitano et al. 2014; Huang et al. 2014;
728 Richards et al. 2016; Gélin et al. 2017, 2018; Arrigoni et al. 2018). During the last decade, combined morpho-
729 molecular approaches described new genera and species endemic to the northern and/or western Indian Ocean, thus
730 increasing the coral biodiversity of this area (Benzoni and Stefani 2012; Benzoni et al. 2012; Terraneo et al. 2014;
731 Arrigoni et al. 2015, 2016b, 2016c). Therefore, it is becoming increasingly clear that, although species richness is
732 highest in the Coral Triangle, the Indian Ocean displays a higher number of endemisms possibly as the result of a
733 combination of higher speciation rates and lower extinction rates in its peripheral areas such as the Red Sea and the
734 western Indian Ocean (Huang et al. 2018; McFadden et al. 2019).

735 The integrated approach we adopted to define species boundaries within *Leptastrea* corroborated the above
736 mentioned findings and provided a new perspective on the biogeography of the genus. So far, all the analyzed species
737 have been considered to be widely distributed throughout the Indo-Pacific, from the Red Sea to the Central Pacific
738 (distribution maps in Veron 2000). Our results showed, however, that only *L. purpurea* and *L. transversa* display such
739 a widespread geographic distribution without intraspecific genomic breaks. Conversely, *L. gibbosa* sp. n. only occurs
740 in the Western and central Pacific Ocean, *L. magaloni* sp. n. seems to be an endemism of the Mozambique Channel
741 (although the species actual distribution could extend further in the SWIO), whereas *L. bottae* and *L. inaequalis* occur
742 in the Red Sea and Arabian Sea, and then extend in various localities of the Indian Ocean. Therefore, *Leptastrea*
743 actually displays its peak of diversity and endemism in the western and northern Indian Ocean (Fig. 6b). These results
744 confirm the evolutionary distinctiveness of corals occurring in the northern and western Indian Ocean (Obura 2012,
745 2016). Interestingly, distributional data of extant coral species seem to indicate the presence of two distinct centers of
746 diversity in this basin which are the northern Mozambique Channel and the Red Sea (Obura 2012; Veron et al. 2015).
747 Fossils and phylogenetic data suggest the presence of multiple centers of origin in this area and, in particular, a first
748 one in the Paleogene Tethys Sea and a second one in the Neogene Red Sea and Arabian Sea (Obura 2016; Arrigoni et
749 al. 2019). Important tectonic changes occurred in what is now the Indian Ocean during both the Paleogene and the
750 Neogene and may have promoted isolation and speciation events (Schettino and Turco 2011; Keith et al. 2013; Obura
751 2016). Unfortunately, in the absence of a reliable fossil record for *Leptastrea* or estimates of its lineage ages, we
752 cannot currently test whether the three species of *Leptastrea* restricted to the Indian Ocean originated in the Paleogene
753 or Neogene.

Acknwledgements This project was supported by funding from KAUST (award # FCC/1/1973-21 and baseline research funds to MLB). This research was undertaken in accordance with the policies and procedures of KAUST. Permissions relevant for KAUST to undertake the research have been obtained from the applicable governmental agencies in the Kingdom of Saudi Arabia. We wish to thank A Gusti (KAUST), the captain and crew of the MV Dream-Master, and the KAUST Coastal and Marine Resources Core Lab for fieldwork logistics in the Red Sea. In Yemen, fieldwork organization, logistics and sampling permits from the relevant authorities were possible hanks to the collaboration of E Dutrieux (Creocean), CH Chaineau (Total SA), R Hirst, and M Abdul Aziz (YLNG). We are grateful to E Karsenti (EMBL) and E Bougois (Tara Expeditions), the OCEANS Consortium for allowing sampling during the Tara Oceans expedition in Djibouti and Mayotte. We thank the commitment of the following people and additional sponsors who made this singular expedition possible: CNRS, EMBL, Genoscope/CEA, VIB, Stazione Zoologica Anton Dohrn, UNIMIB, ANR (projects POSEIDON/ANR-09-BLAN-0348, BIOMARKS/ANR-08-BDVA-003, PROMETHEUS/ANR-09-GENM-031, and TARA-GIRUS/ANR-09-PCS-GENM-218), EU FP7 (MicroB3/No.287589), FWO, BIO5, Biosphere 2, agnès b., the Veolia Environment Foundation, Region Bretagne, World Courier, Illumina, Cap L'Orient, the EDF Foundation EDF Diversiterre, FRB, the Prince Albert II de Monaco Foundation, Etienne Bourgois, the Tara schooner, and its captain and crew. Tara Oceans would not exist without continuous support from 23 institutes (http://oceans.taraexpeditions.org). This article is contribution number **XX** of the Tara Oceans Expedition 2009–2012. New Caledonia data and specimens were obtained during the IRD CORALCAL1 (http://dx.doi.org/10.17600/7100020), CORALCAL2 (http://dx.doi.org/10.17600/8100050), CORALCAL3 (http://dx.doi.org/10.17600/9100010), CORALCAL4 (http://dx.doi.org/10.17600/12100060), BIBELOT (http://dx.doi.org/10.17600/14003700), and CORALCAL5 (http://dx.doi.org/10.17600/15004300) expeditions on the RV Alis. We are grateful to the chief scientists and cruise organisers C Payri (IRD), C Fauvelot (IRD) for invitation and financial support to join and valuable help with sampling authorisations. Material from Madagascar was collected during the MAD (http://dx.doi.org/10.17600/16004700) expedition on the RV Antea organised by H Magalon (ULR). The MADANG expedition specimens were obtained during the "Our Planet Reviewed" Papua Niugini expedition (http://dx.doi.org/10.17600/12100070) organised by Muséum National d'Histoire Naturelle (MNHN), Pro Natura International (PNI), Institut de Recherche pour le Développement (IRD),

782 and University of Papua New Guinea (UPNG), Principal Investigators P Bouchet, C Payri, and S Samadi. The
783 organizers acknowledge funding from the Total Foundation, Prince Albert II of Monaco Foundation, Fondation EDF,
784 Stavros Niarchos Foundation, and Entrepose Contracting, and in-kind support from the Divine Word University
785 (DWU). Material from Kavieng, PNG, was sampled during the KAVIENG Expedition
786 (https://doi.org/10.17600/14004400). The expedition operated under a permit delivered by the Papua New Guinea
787 Department of Environment and Conservation. Material from the Coral Sea, Australia, was sampled in under Permit
788 No. AU-COM2018-437. The authors wish to thank A.H. Baird (JCU), M. Pratchett (JCU), and Hugo Harrison (JCU)
789 and the relevant staff at Parks Australia. We are grateful to A. Andouche (MNHN), M. Castellin (MNHN), P. Lozouet
790 (MNHN), C. Lüter (ZMB), T. Bridge (MTQ), P. Muir (MTQ), M. Lowe (NHM) and A. Cabrinovic (NHM) for
791 allowing the study of the museum reference collections. The views expressed are purely those of the writers and may
792 not in any circumstance be regarded as stating an official position of the European Commission. We are grateful to
793 Z.H. Forsman (UH Manoa) and one anonymous reviewer for their useful corrections and suggestions.
794
795 **Compliance with ethical standards**
796
797 **Conflict of interest** On behalf of all authors, the corresponding author states that there is no conflict of intest.
798
799 **References**
800 Al Tawaha M, Benzoni F, Eid E, Abu Awali A (2019) The hard corals of Jordan, a field guide. Amman, Jordan, the
801 Royal Marine Conservation Society of Jordan
802 Andrews KR, Good JM, Miller MR, Luikart G, Hohenlohe PA (2016) Harnessing the power of RADseq for ecological
803 and evolutionary genomics. Nat Rev Genet 17:81–92
804 Arrigoni R, Stefani F, Pichon M, Galli P, Benzoni F (2012) Molecular phylogeny of the robust clade (Faviidae,
805 Mussidae, Merulinidae, and Pectiniidae): an Indian Ocean perspective. Mol Phylogenet Evol 65:183–193
806 Arrigoni R, Berumen ML, Terraneo TI, Caragnano A, Bouwmeester J, Benzoni F (2015) Forgotten in the taxonomic
807 literature: resurrection of the scleractinian coral genus *Sclerophyllia* (Scleractinia, Lobophylliidae) from the
808 Arabian Peninsula and its phylogenetic relationships. Syst Biodivers 13:140–163
809 Arrigoni R, Benzoni F, Terraneo TI, Caragnano A, Berumen ML (2016a) Recent origin and semi-permeable species
810 boundaries in the scleractinian coral genus *Stylophora* from the Red Sea. Sci Rep 6:34612
811 Arrigoni R, Berumen ML, Chen CA, Terraneo TI, Baird AH, Payri C, Benzoni F (2016b) Species delimitation in the
812 reef coral genera *Echinophyllia* and *Oxypora* (Scleractinia, Lobophylliidae) with a description of two new species.
813 Mol Phylogenet Evol 105:146–159
814 Arrigoni R, Benzoni F, Huang D, Fukami H, Chen CA, Berumen ML, Hoogenboom M, Thomson DP, Hoeksema
815 BW, Budd AF, Zayasu Y, Terraneo TI, Kitano YF, Benzoni F (2016c) When forms meet genes: revision of the
816 scleractinian genera *Micromussa* and *Homophyllia* (Lobophylliidae) with a description of two new species and
817 one new genus. Contrib Zool 85:387–422
818 Arrigoni R, Maggioni D, Montano S, Hoeksema BW, Seveso D, Shlesinger T, Terraneo TI, Tietbohl MD, Berumen
819 ML (2018) An integrated morpho-molecular approach to delineate species boundaries of *Millepora* from the Red
820 Sea. Coral Reefs 37:967–984

821 Arrigoni R, Berumen ML, Stolarski J, Terraneo TI, Benzoni F (2019) Uncovering hidden coral diversity: a new cryptic
822 lobophylliid scleractinian from the Indian Ocean. Cladistics 35:301–328
823 Avise JC, Robinson TJ, Kubatko L (2008) Hemiplasy: a new term in the lexicon of phylogenetics. Syst Biol 57:503–
824 507
825 Baird NA, Etter PD, Atwood TS, Currey MC, Shiver AL, Lewis ZA, Selker EU, Cresko WA, Johnson EA (2008)
826 Rapid SNP discovery and genetic mapping using sequenced RAD markers. PloS ONE 3:e3376
827 Benzoni F, Stefani F (2012) *Porites fontanesii*, a new species of hard coral (Scleractinia, Poritidae) from the southern
828 Red Sea, the Gulf of Tadjoura, and the Gulf of Aden. Zootaxa 3447:56–68
829 Benzoni F, Arrigoni R, Stefani F, Stolarski J (2012) Systematics of the coral genus *Craterastrea* (Cnidaria, Anthozoa,
830 Scleractinia) and description of a new family through combined morphological and molecular analyses. Syst
831 Biodivers 10:417–433
832 Berumen ML, Arrigoni R, Bouwmeester J, Terraneo TI, Benzoni F (2019) Corals of the Red Sea. In: Voolstra CR,
833 Berumen ML (eds) Coral Reefs of the Red Sea. Springer Cham, Berlin, pp 123–155
834 Boero F (2001) Light after dark: the partnership for enhancing expertise in taxonomy. Trends Ecol. Evol. 16:266
835 Bolger AM, Lohse M, Usadel B (2014) Trimmomatic: a flexible trimmer for Illumina sequence data. Bioinformatics
836 30:2114–2120
837 Bouckaert RR (2010) DensiTree: making sense of sets of phylogenetic trees. Bioinformatics 26:1372–1373
838 Bouckaert R, Heled J, Kühnert D, Vaughan T, Wu CH, Xie D, Suchards MA, Rambaut A, Drummond AJ (2014)
839 BEAST 2: a software platform for Bayesian evolutionary analysis. PLoS Comput Biol 10:e1003537
840 Bryant D, Bouckaert R, Felsenstein J, Rosenberg NA, Roy-Choudhury A (2012) Inferring species trees directly from
841 biallelic genetic markers: bypassing gene trees in a full coalescent analysis. Mol Biol Evol 29:1917–1932
842 Budd AF, Fukami H, Smith ND, Knowlton N (2012) Taxonomic classification of the reef coral family Mussidae
843 (Cnidaria: Anthozoa: Scleractinia). Zool J Linnean Soc 166:465–529
844 Cariou M, Duret L, Charlat S (2013) Is RAD-seq suitable for phylogenetic inference? An *in silico* assessment and
845 optimization. Ecol Evol 3:846–852
846 Carlon DB, Budd AF (2002) Incipient speciation across a depth gradient in a scleractinian coral? Evolution 56:2227–
847 2242
848 Carlon DB, Budd AF, Lippé C, Andrew RL (2011) The quantitative genetics of incipient speciation: heritability and
849 genetic correlations of skeletal traits in populations of diverging *Favia fragum* ecomorphs. Evolution 65:3428–
850 3447
851 Chevalier JP (1975) Les scléractiniaires de la mélanésie francaise (Nouvelle- Calédonie, lies Chesterfield, lies
852 Loyauté, Nouvelles-Hébrides). Expédition Francaise Sur les Récifs Coralliens de la Nouvelle-Calédonie,
853 Deuxieme Partie. Fond Singer-Polignac, Paris
854 Crossland C (1952) Madreporaria, Hydrocorallinae, *Heliopora* and *Tubipora*. Sci. Rep. Great Barrier Reef Exped.
855 1928-29. Bull Br Mus Nat Hist Zool 6:85–257
856 Danecek P, Auton A, Abecasis G, Albers CA, Banks E, DePristo MA, Handsaker RE, Lunter G, Marth GT, Sherry
857 ST, McVean G, Durbin R, 1000 Genome Project Data Processing Subgroup (2011) The variant call format and
858 VCFtools. Bioinformatics 27:2156–2158
859 Davey JW, Blaxter ML (2010) RADSeq: next-generation population genetics. Brief Funct Genomics 9:416–423
860 Dimond JL, Gamblewood SK, Roberts SB (2017) Genetic and epigenetic insight into morphospecies in a reef coral.
861 Mol Ecol 26:5031-5042
862 Drummond AJ, Bouckaert RR (2015) Bayesian evolutionary analysis with BEAST. Harvard University Press,
863 Cambridge
864 Eaton DAR, Ree RH (2013) Inferring phylogeny and introgression using RADseq data: an example from flowering
865 plants (*Pedicularis*: Orobanchaceae). Syst Biol 62:689–706
866 Eaton DA, Spriggs EL, Park B, Donoghue MJ (2017) Misconceptions on missing data in RAD-seq phylogenetics with
867 a deep-scale example from flowering plants. Syst Biol 66:399–412
868 Flot JF, Blanchot J, Charpy L, Cruaud C, Licuanan WY, Nakano Y, Payri C, Tillier S (2011) Incongruence between
869 morphotypes and genetically delimited species in the coral genus *Stylophora*: phenotypic plasticity, morphological
870 convergence, morphological stasis or interspecific hybridization? BMC Ecol 11:22
871 Forsman ZH, Barshis DJ, Hunter CL, Toonen RJ (2009) Shape-shifting corals: molecular markers show morphology
872 is evolutionarily plastic in *Porites*. BMC Evol Biol 9:45
873 Forsman ZH, Concepcion GT, Haverkort RD, Shaw RW, Maragos JE, Toonen RJ (2010) Ecomorph or endangered
874 coral? DNA and microstructure reveal Hawaiian species complexes: *Montipora dilatata/flabellata/turgescens* &
875 *M. patula/verrilli*. PLoS ONE 5:e15021

876 Forsman ZH, Knapp ISS, Tisthammer K, Eaton DAR, Belcaid M, Toonen RJ (2017) Coral hybridization or phenotypic
877 variation? Genomic data reveal gene flow between *Porites lobata* and *P. compressa*. Mol Phylogenet Evol
878 111:132–148
879 Frade PR, Reyes-Nivia MC, Faria J, Kaandorp JA, Luttikhuizen PC, Bak RPM (2010) Semi-permeable species
880 boundaries in the coral genus *Madracis*: introgression in a brooding coral system. Mol Phylogenet Evol 57:1072–
881 1090
882 Fukami H, Chen CA, Budd AF, Collins A, Wallace C, Chuang YY, Chen C, Dai CF, Iwao K, Sheppard C, Knowlton
883 N (2008) Mitochondrial and nuclear genes suggest that stony corals are monophyletic but most families of stony
884 corals are not (Order Scleractinia, Class Anthozoa, Phylum Cnidaria). PloS ONE 3:e3222
885 García-Roselló E, Guisande C, Manjarrés-Hernández A, González-Dacosta J, Heine J, Pelayo-Villami P, González-
886 Vilas L, Vari RP, Vaamonde A, Granado-Lorencio C, Lobo JM (2015) Can we derive macroecological patterns
887 from primary Global Biodiversity Information Facility data? Global Ecol Biogeog 24:335–347
888 Garrison E, Marth G (2012) Haplotype-based variant detection from short-read sequencing. arXiv Prepr
889 arXiv12073907:1–9
890 Gautier M, Gharbi K, Cezard T, Foucaud J, Kerdelhué C, Pudlo P, Cornuet JM, Estoup A (2013) The effect of RAD
891 allele dropout on the estimation of genetic variation within and between populations. Mol Ecol 22:3165–3178
892 Gélin P, Postaire B, Fauvelot C, Magalon H (2017) Reevaluating species number, distribution and endemism of the
893 coral genus *Pocillopora* Lamarck, 1816 using species delimitation methods and microsatellites. Mol Phylogenet
894 Evol 109:430–446
895 Gélin P, Fauvelot C, Bigot L, Baly J, Magalon H (2018) From population connectivity to the art of striping Russian
896 dolls: the lessons from *Pocillopora* corals. Ecol Evol 8:1411–1426
897 Gori K, Suchan T, Alvarez N, Goldman N, Dessimoz C (2016) Clustering genes of common evolutionary history.
898 Mol Biol Evol 33:1590–1605
899 Hellberg ME (2006) No variation and low synonymous substitution rates in coral mtDNA despite high nuclear
900 variation. BMC Evol Biol 6:24
901 Herrera S, Shank TM (2016) RAD sequencing enables unprecedented phylogenetic resolution and objective species
902 delimitation in recalcitrant divergent taxa. Mol Phylogenet Evol 100:70–79
903 Hoeksema BW (2007) Delineation of the Indo-Malayan centre of maximum marine biodiversity: the coral triangle.
904 In: Renema W (ed) Biogeography, time and place: distributions, barriers and islands. Springer Cham, Berlin, pp
905 117–178
906 Hoeksema BW, Cairns S (2019) World List of Scleractinia. *Leptastrea* Milne Edwards & Haime, 1849. Accessed
907 through: World Register of Marine Species at: http://www.marinespecies.org/aphia.php?p=taxdetails&id=204278
908 on 2019-12-04
909 Hou Y, Nowak MD, Mirré V, Bjorå CS, Brochmann C, Popp M (2015) Thousands of RAD-seq loci fully resolve the
910 phylogeny of the highly disjunct arctic-alpine genus *Diapensia* (Diapensiaceae). PLoS One 10: e0140175
911 Huang D, Benzoni F, Fukami H, Knowlton N, Smith ND, Budd AF (2014) Taxonomic classification of the reef coral
912 families Merulinidae, Montastraeidae, and Diploastraeidae (Cnidaria: Anthozoa: Scleractinia). Zool J Linnean Soc
913 171:277–355
914 Huang D, Benzoni F, Arrigoni R, Baird AH, Berumen ML, Bouwmeester J, Chou LM, Fukami H, Licuanan WY,
915 Lovell ER, Mieri R, Todd PA, Budd AF, Meier R (2014) Towards a phylogenetic classification of reef corals: the
916 Indo-Pacific genera *Merulina*, *Goniastrea* and *Scapophyllia* (Scleractinia, Merulinidae). Zool Scripta 43:531–548
917 Huang D, Goldberg EE, Chou LM, Roy K (2018) The origin and evolution of coral species richness in a marine
918 biodiversity hotspot. Evolution 72:288–302
919 Hughes TP, Barnes ML, Bellwood DR, Cinner JE, Cumming GS, Jackson JB, Kleypas J, van de Leemput IA, Lough
920 JM, Morrison TH, Palumbi SR, van Nes EH, Scheffer M (2017) Coral reefs in the Anthropocene. Nature 546:82–
921 90
922 Hughes TP, Anderson KD, Connolly SR, Heron SF, Kerry JT, Lough JM., Baird AH, Baum JK, Berumen ML, Bridge
923 TC, Claar DC, Eakin CM, Gilmour JP, Graham NAJ, Harrison H, Hobbs JPA, Hoey AS, Hoogenboom M, Lowe
924 RJ, McCulloch MT, Pandolfi JM, Pratchett M, Schoepf V, Torda G, Wilson SK (2018) Spatial and temporal
925 patterns of mass bleaching of corals in the Anthropocene. Science 359:80–83
926 Hughes TP, Kerry JT, Baird AH, Connolly SR, Chase TJ, Dietzel A, Hill T, Hoey AS, Hoogenboom MO, Jacobson
927 M, Kerswell A, Madin JS, Mieog A, Paley AS, Pratchett MS, Torda G, Woods RM (2019) Global warming impairs
928 stock–recruitment dynamics of corals. Nature 568:387–390
929 Johnson CN, Balmford A, Brook BW, Buettel JC, Galetti M, Guangchun L, Wilmshurst JM (2017) Biodiversity losses
930 and conservation responses in the Anthropocene. Science 356:270–275

931 Johnston EC, Forsman ZH, Flot JF, Schmidt-Roach S, Pinzón JH, Knapp IS, Toonen RJ (2017) A genomic glance
932 through the fog of plasticity and diversification in *Pocillopora*. Sci Rep 7:5991.
933 Kass RE, Raftery AE (1995) Bayes factors. J Am Stat Assoc 90:773–795
934 Katoh K, Standley DM (2013) MAFFT multiple sequence alignment software version 7: improvements in
935 performance and usability. Mol Biol Evol 30:772–780
936 Keith SA, Baird AH, Hughes TP, Madin JS, Connolly SR (2013) Faunal breaks and species composition of Indo-
937 Pacific corals: the role of plate tectonics, environment and habitat distribution. Proc R Soc Lond 280:20130818
938 Klunzinger CB (1879) Die Korallenthiere des Rothen Meeres, 3. Gutmann, Berlin
939 Kitahara MV, Fukami H, Benzoni F, Huang D (2016) The new systematics of Scleractinia: integrating molecular and
940 morphological evidence. In: Dubinsky Z, Goffredo S (eds) The Cnidaria, past, present and future. Springer Cham,
941 Berlin, pp 41–59
942 Kitano YF, Benzoni F, Arrigoni R, Shirayama Y, Wallace CC, Fukami H (2014) A phylogeny of the family Poritidae
943 (Cnidaria, Scleractinia) based on molecular and morphological analyses. PLoS ONE 9:e98406
944 Kitchen SA, Crowder CM, Poole AZ, Weis VM, Meyer E (2015) De novo assembly and characterization of four
945 anthozoan (phylum Cnidaria) transcriptomes. G3: Genes Genom Genet 5:2441–2452
946 Knapp IS, Puritz JB, Bird CE, Whitney JL, Sudek M, Forsman ZH, Toonen RJ (2016) ezRAD-an accessible next-
947 generation RAD sequencing protocol suitable for non-model organisms v3. 1. Protocols io Life Sciences Protocol
948 Repository. http://dx.doi.org/10.17504/protocols.io.e9pbh5n
949 Knowlton N (2001) The future of coral reefs. Proc Nat Acad Sci USA 98:5419–5425
950 Kubatko LS, Degnan JH (2007) Inconsistency of phylogenetic estimates from concatenated data under coalescence.
951 Syst Biol 56:17–24
952 Lanfear R, Frandsen PB, Wright AM, Senfeld T, Calcott B (2016) PartitionFinder 2: new methods for selecting
953 partitioned models of evolution for molecular and morphological phylogenetic analyses. Mol Biol Evol 34:772–
954 773
955 Langmead B, Salzberg SL (2012) Fast gapped-read alignment with Bowtie 2. Nature Methods 9:357
956 Leaché AD, Fujita MK, Minin VN, Bouckaert RR (2014) Species delimitation using genome-wide SNP data. Syst
957 Biol 63:534–542
958 Li H, Durbin R (2009) Fast and accurate short read alignment with Burrows–Wheeler transform. Bioinformatics
959 25:1754–1760
960 Li H, Handsaker B, Wysoker A, Fennell T, Ruan J, Homer N, Marth G, Abecasis G, Durbin R, 1000 Genome Project
961 Data Processing Subgroup (2009) The Sequence Alignment/Map format and SAMtools. Bioinformatics 25:2078–
962 2079
963 Lischer HE, Excoffier L (2011) PGDSpider: an automated data conversion tool for connecting population genetics
964 and genomics programs. Bioinformatics 28:298–299
965 Massatti R, Reznicek AA, Knowles LL (2016) Utilizing RADseq data for phylogenetic analysis of challenging
966 taxonomic groups: a case study in *Carex* sect. *Racemosae*. Am J Bot 103:337–347
967 Matthai G (1914) No. I. –A revision of the recent colonial Astræidæ possessing distinct corallites. Trans Linn Soc
968 Lond 17:1–140
969 McCauley DJ, Pinsky ML, Palumbi SR, Estes JA, Joyce FH, Warner RR (2015) Marine defaunation: animal loss in
970 the global ocean. Science 347:1255641
971 McFadden CS, Haverkort-Yeh R, Reynolds AM, Halàsz A, Quattrini AM, Forsman ZH, Benayahu Y, Toonen RJ
972 (2017) Species boundaries in the absence of morphological, ecological or geographical differentiation in the Red
973 Sea octocoral genus *Ovabunda* (Alcyonacea: Xeniidae). Mol Phylogenet Evol 112:174–184
974 McFadden CS, Gonzalez A, Imada R, Shi SS, Hong P, Ekins M, Benayahu Y (2019) Molecular operational taxonomic
975 units reveal restricted geographic ranges and regional endemism in the Indo-Pacific octocoral family Xeniidae. J
976 Biogeogr 46:992–1006
977 Metzker ML (2010) Sequencing technologies–the next generation. Nat Rev Genet 11:31–46
978 Miller MA, Pfeiffer W, Schwartz T (2010) Creating the CIPRES Science Gateway for inference of large phylogenetic
979 trees. Proceedings of the Gateway Computing Environments Workshop, New Orleans
980 Miller MR, Dunham JP, Amores A, Cresko WA, Johnson EA (2007) Rapid and cost-effective polymorphism
981 identification and genotyping using restriction site associated DNA (RAD) markers. Genome Res 17:240–9248
982 Milne Edwards M, Haime J (1849) Recherches sur les polypiers; 4eme mémoire. Monographie des Astréides. Ann
983 Sci Nat 3:95–197
984 Nishihira M, Veron JEN (1995) Hermatypic Corals of Japan. Kaiyusha, Tokyo
985 Obura DO (2012) The diversity and biogeography of Western Indian Ocean reef-building corals. PloS ONE 7:e45013

Obura DO (2016) An Indian Ocean centre of origin revisited: Palaeogene and Neogene influences defining a biogeographic realm. J Biogeogr 43:229–242
Pante E, Abdelkrim J, Viricel A, Gey D, France SC, Boisselier MC, Samadi S (2015) Use of RAD sequencing for delimiting species. Heredity 114:450–459
Paz-García DA, Hellberg ME, García-de-León FJ, Balart EF (2015) Switch between morphospecies of *Pocillopora* corals. Amer Nat 186:434–440
Pinzón JH, Sampayo E, Cox E, Chauka LJ, Chen CA, Voolstra CR, LaJeunesse TC (2013) Blind to morphology: genetics identifies several widespread ecologically common species and few endemics among Indo-Pacific cauliflower corals (*Pocillopora*, Scleractinia). J Biogeogr 40:1595–1608
Prada C, DeBiasse MB, Neigel JE, Yednock B, Stake JL, Forsman ZH, Baums IB, Hellberg ME (2014) Genetic species delineation among branching Caribbean *Porites* corals. Coral Reefs 33:1019–1030
Pratchett MS, Caballes CF, Wilmes JC, Matthews S, Mellin C, Sweatman H, Nadler LE, Brodie J, Thmpson CA, Hoey J, Bos AR, Byrne M, Messmer V, Fortunato SA, Chen CCM, Buck ACE, Barbcok RC, Uthicke S (2017) Thirty years of research on crown-of-thorns starfish (1986–2016): scientific advances and emerging opportunities. Diversity 9:41
Puritz JB, Hollenbeck CM, Gold JR (2014) dDocent: a RADseq, variant-calling pipeline designed for population genomics of non-model organisms. PeerJ 2:e431
Quattrini AM, Wu T, Soong K, Jeng MS, Benayahu Y, McFadden CS (2019) A next generation approach to species delimitation reveals the role of hybridization in a cryptic species complex of corals. BMC Evol Biol 19:116
Quinlan AR, Hall IM (2010) BEDTools: a flexible suite of utilities for comparing genomic features. Bioinformatics 26:841–842
Rambaut A, Drummond AJ, Xie D, Baele G, Suchard MA (2018) Posterior summarization in Bayesian phylogenetics using Tracer 1.7. Syst Biol 67:901–904
Rancilhac L, Goudarzi F, Gehara M, Hemami MR, Elmer KR, Vences M, Steinfarz S (2019) Phylogeny and species delimitation of near Eastern *Neurergus* newts (Salamandridae) based on genome-wide RADseq data analysis. Mol Phylogenet Evol 133:1890–1897
Richards ZT, Berry O, Van Oppen MJ (2016) Cryptic genetic divergence within threatened species of *Acropora* coral from the Indian and Pacific Oceans. Conserv Genet 17:577–591
Roberts CM, McClean CJ, Veron JEN, Hawkins JP, Allen GR, McAllister DE, Mittermeier CG, Schueler FW, Spalding M, Weels F, Vynne C, Werner TB (2002) Marine biodiversity hotspots and conservation priorities for tropical reefs. Science 295:1280–1284
Rubin BE, Ree RH, Moreau CS (2012) Inferring phylogenies from RAD sequence data. PloS ONE 7:e33394
Rueden CT, Schindelin J, Hiner MC, DeZonia BE, Walter AE, Arena ET, Eliceiri KW (2017) ImageJ2: ImageJ for the next generation of scientific image data. BMC Bioinformatics 18:529
Sanderson MJ, Driskell AC, Ree RH, Eulenstein O, Langley S (2003) Obtaining maximal concatenated phylogenetic data sets from large sequence databases. Mol Biol Evol 20:1036-1042
Sargent TD, Jamrich M, Dawid IB (1986) Cell interactions and the control of gene activity during early development of *Xenopus laevis*. Dev Biol 114:238–246
Scheer G, Pillai CSG (1974) Report on the Scleractinia from the Nicobar Islands. Zoologica 42:1–198
Scheer G, Pillai CSG (1983) Report on the stony corals from the Red Sea. Zoologica 45:1–184
Schettino A, Turco E (2011) Tectonic history of the western Tethys since the Late Triassic. Geol Soc Am Bull 123:89–105
Schmidt-Roach S, Miller KJ, Lundgren P, Andreakis N (2014) With eyes wide open: a revision of species within and closely related to the *Pocillopora damicornis* species complex (Scleractinia; Pocilloporidae) using morphology and genetics. Zool J Linnean Soc 170:1–33
Shearer TL, Van Oppen MJH, Romano SL, Wörheide G (2002). Slow mitochondrial DNA sequence evolution in the Anthozoa (Cnidaria). Mol Ecol 11:2475–2487
Sheppard CRC, Sheppard ALS (1991) Corals and coral communities of Saudi Arabia. Fauna of Arabia 12:1–170
Stamatakis A (2014) RAxML version 8: a tool for phylogenetic analysis and post-analysis of large phylogenies. Bioinformatics 30:1312–1313
Stefani F, Benzoni F, Yang SY, Pichon M, Galli P, Chen CA (2011) Comparison of morphological and genetic analyses reveals cryptic divergence and morphological plasticity in *Stylophora* (Cnidaria, Scleractinia). Coral Reefs 30:1033-1049
Stobie CS, Cunningham MJ, Oosthuizen CJ, Bloomer P (2019) Finding stories in noise: mitochondrial portraits from RAD data. Mol Ecol Resour 19:191–205

1041 Suchan T, Espíndola A, Rutschmann S, Emerson BC, Gori K, Dessimoz C, Arrigo N, Ronikier M, Alvarez N (2017)
1042 Assessing the potential of RAD-sequencing to resolve phylogenetic relationships within species radiations: the fly
1043 genus *Chiastocheta* (Diptera: Anthomyiidae) as a case study. Mol Phylogenet Evol 114:189–198
1044 Terraneo TI, Berumen ML, Arrigoni R, Waheed Z, Bouwmeester J, Caragnano A, Stefani F, Benzoni F (2014)
1045 *Pachyseris inattesa* sp. n. (Cnidaria, Anthozoa, Scleractinia): a new reef coral species from the Red Sea and its
1046 phylogenetic relationships. ZooKeys 433:1–30
1047 Terraneo TI, Benzoni F, Arrigoni R, Berumen ML (2016) Species delimitation in the coral genus *Goniopora*
1048 (Scleractinia, Poritidae) from the Saudi Arabian Red Sea. Mol Phylogenet Evol 102:278–294
1049 Terraneo TI, Arrigoni R, Benzoni F, Forsman ZH, Berumen ML (2018a) Using ezRAD to reconstruct the complete
1050 mitochondrial genome of *Porites fontanesii* (Cnidaria: Scleractinia). Mitochondrial DNA B Resour 3:173–174
1051 Terraneo TI, Arrigoni R, Benzoni F, Forsman ZH, Berumen ML (2018b) The complete mitochondrial genome of
1052 *Porites harrisoni* (Cnidaria: Scleractinia) obtained using next-generation sequencing. Mitochondrial DNA B
1053 Resour 3:286–287
1054 Todd PA (2008) Morphological plasticity in scleractinian corals. Biol Rev 83:315–337
1055 Toonen RJ, Puritz JB, Forsman ZH, Whitney JL, Fernandez-Silva I, Andrews KR, Bird CE (2013) ezRAD: a
1056 simplified method for genomic genotyping in non-model organisms. PeerJ 1:e203
1057 Van Oppen MV, Willis BL, Vugt HV, Miller DJ (2000) Examination of species boundaries in the *Acropora*
1058 *cervicornis* group (Scleractinia, Cnidaria) using nuclear DNA sequence analyses. Mol Ecol 9:1363–1373
1059 Vaughan TW (1918) Some shoal-water corals from Murray Islands, Cocos Keeling Islands ana Fanning Islands. Pap
1060 Dep Mar Biol Carnegie Inst Wash 9:51–234
1061 Veron JEN, Pichon M, Wijsman-Best M (1977) Scleractinia of eastern Australia. Part II. Families Faviidae,
1062 Trachyphylliidae. Australian Institute of Marine Science, Townsville
1063 Veron JEN (2000) Corals of the World. Australian Institute of Marine Science, Townsville
1064 Veron JEN (2002) New species described in corals of the world. Australian Institute of Marine Science, Townsville
1065 Veron JEN, Stafford-Smith M, DeVantier L, Turak E (2015) Overview of distribution patterns of zooxanthellate
1066 Scleractinia. Front Mar Sci 1:81
1067 Verrill A (1867) Synopsis of the polyps and corals of the North Pacific Exploring Expedition, with descriptions of
1068 some additional species from the West Coast of North America. III Madreporaria. Proc Essex Inst Salem 5:33–50
1069 Vollmer SV, Palumbi SR (2004) Testing the utility of internally transcribed spacer sequences in coral phylogenetics.
1070 Mol Ecol 13:2763–2772
1071 Wagner CE, Keller I, Wittwer S, Selz OM, Mwaiko S, Greuter L, Sivasundar A, Seehaunsen O (2013) Genome-wide
1072 RAD sequence data provide unprecedented resolution of species boundaries and relationships in the Lake Victoria
1073 cichlid adaptive radiation. Mol Ecol 22:787–798
1074 Warner PA, Van Oppen MJ, Willis BL (2015) Unexpected cryptic species diversity in the widespread coral
1075 *Seriatopora hystrix* masks spatial-genetic patterns of connectivity. Mol Ecol 24:2993–3008
1076 Wells JW (1956) Scleractinia. In: Moore RC (ed) Treatise on Invertebrate Paleontology, Part F. Geological Society
1077 of America, Boulder pp F328–F444
1078 Wijsman-Best M (1980) Indo-Pacific coral species belonging to the subfamily Montastreinae Vaughan & Wells, 1943
1079 (Scleractinea – Coelenterata) Part II. The genera *Cyphastrea*, *Leptastrea*, *Echinopora* and *Diploastrea*. Zool
1080 Meded 55:235–263
1081 Willis SC, Hollenbeck CM, Puritz JB, Gold JR, Portnoy DS (2017) Haplotyping RAD loci: an efficient method to
1082 filter paralogs and account for physical linkage. Mol Ecol Resour 17:955–965
1083 Zhang J, Kobert K, Flouri T, Stamatakis A (2013) PEAR: a fast and accurate Illumina Paired-End reAd mergeR.
1084 Bioinformatics 30:614–620
1085

1086 **Figure legends**

1087 **Fig. 1** Skeleton morphology of the *Leptastrea* type specimens (**a, e, i, m, q**) and material examined in this study (**b-d,**

1088 **f-h, j-l, n-p, r-t**): *L. purpurea* (Dana, 1846) (**a** USNM 75; **b-d** UNIMIB GA059), *L. pruinosa* Crossland, 1952 (**e**

1089 BMNH 1934.5.14.630, reproduction of the original illustration; **f-h** UNIMIB GA170), *L. transversa* Klunzinger, 1879

1090 (**e** ZMB Cni 2179; **f-h** UNIMIB DJ297), *L. bottae* (Milne Edwards and Haime, 1849) (**m** MNHN IK-2010-593; **n-p**

1091 KAUST SA044), *L. inaequalis* Klunzinger, 1879 (**q** MNHN IK-2010-596; **n-p** UNIMIB DJ292)

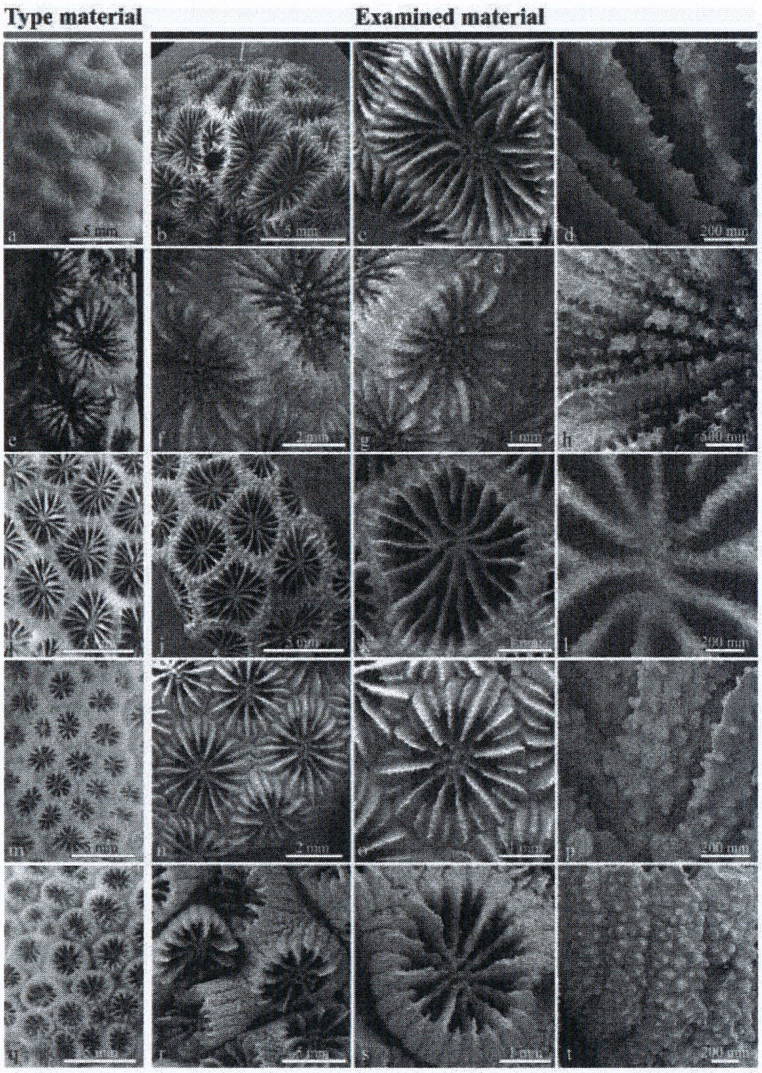

1092

1093 **Fig. 2** *Leptastrea gibbosa* sp. n.: **a** holotype MNHN-IK-2012-9823; **b** IRD HS2344 (black arrows indicates a giant

1094 corallite); **c** IRD HS3740; **d** and **e** corallite arrangement and the characteristic pits and grooves in UNIMIB PFB805

1095 and IRD HS3740, respectively; **f** longitudinal section of IRD HS3740 showing beam-like structures transversally

1096 joining adjacent corallite walls the corallite walls (black arrows) and their longitudinal section (outlined); **g-l** SEM

1097 images of a fragment of the holotype showing **g** detail of the pits among corallites, **h** a side view of the corallum

1098 surface and of the exsert septa, **i** the septa organized in two complete (S1-2) and one incomplete (S3) cycles, **j** the

1099 finely granulated costae, **k** the columella, and **l** a side view of the slightly undulating S1 and S2

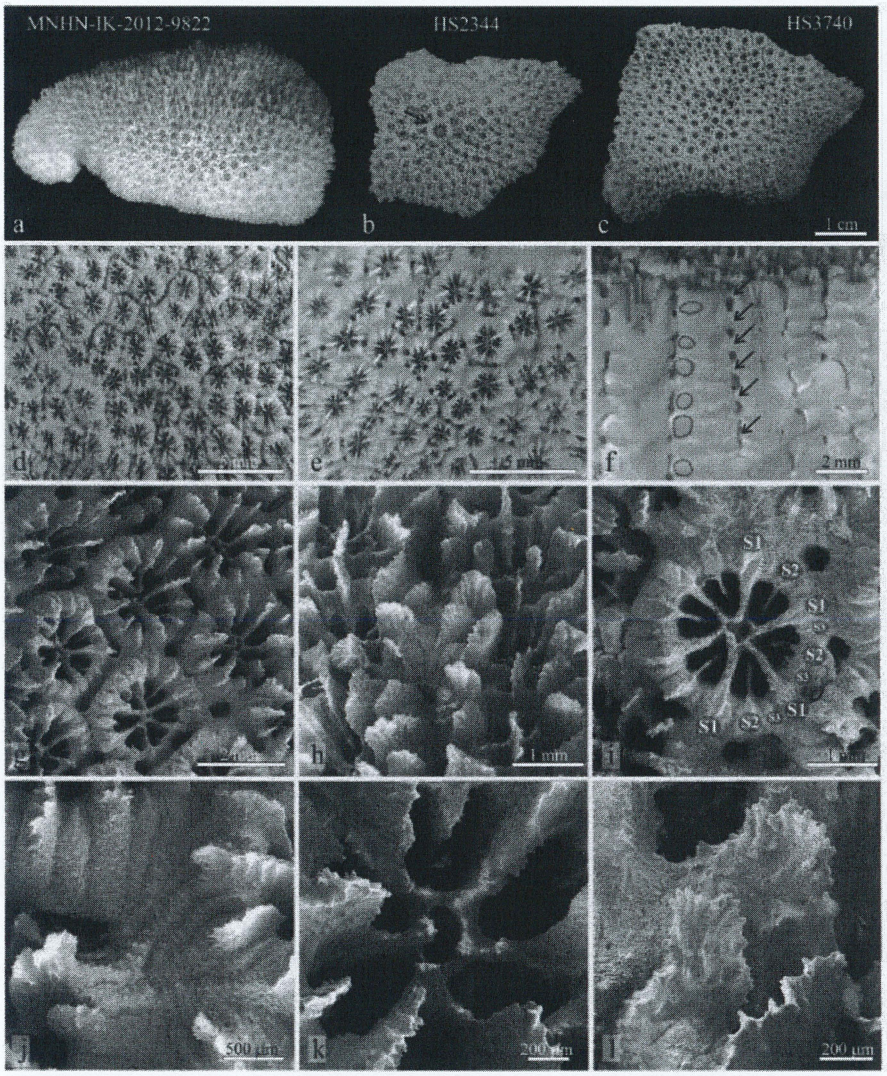

1100

1101 **Fig. 3** *Leptastrea magaloni* sp. n.: **a** holotype MNHN-IK-2012-9823; **b**) IRD MD183, the arrow points at
1102 extratentacular budding; **c** IRD MD225; corallites of **d** the holotype, the arrow points at intratentacular budding, **e**
1103 IRD MD222, **f** IRD MD274; **g** IRD MD260; **h-l** SEM images of a fragment of the holotype showing **h** plocoid
1104 corallites, **i** side view of a corallite and its columella composed of multiple processes, **j** the finely granulated costae,
1105 **k** the septa organized in three complete (S1-4) cycles (arrows point at paddle-shaped structures at the proximal end of
1106 S3), and **l** a side view of S1 and S2

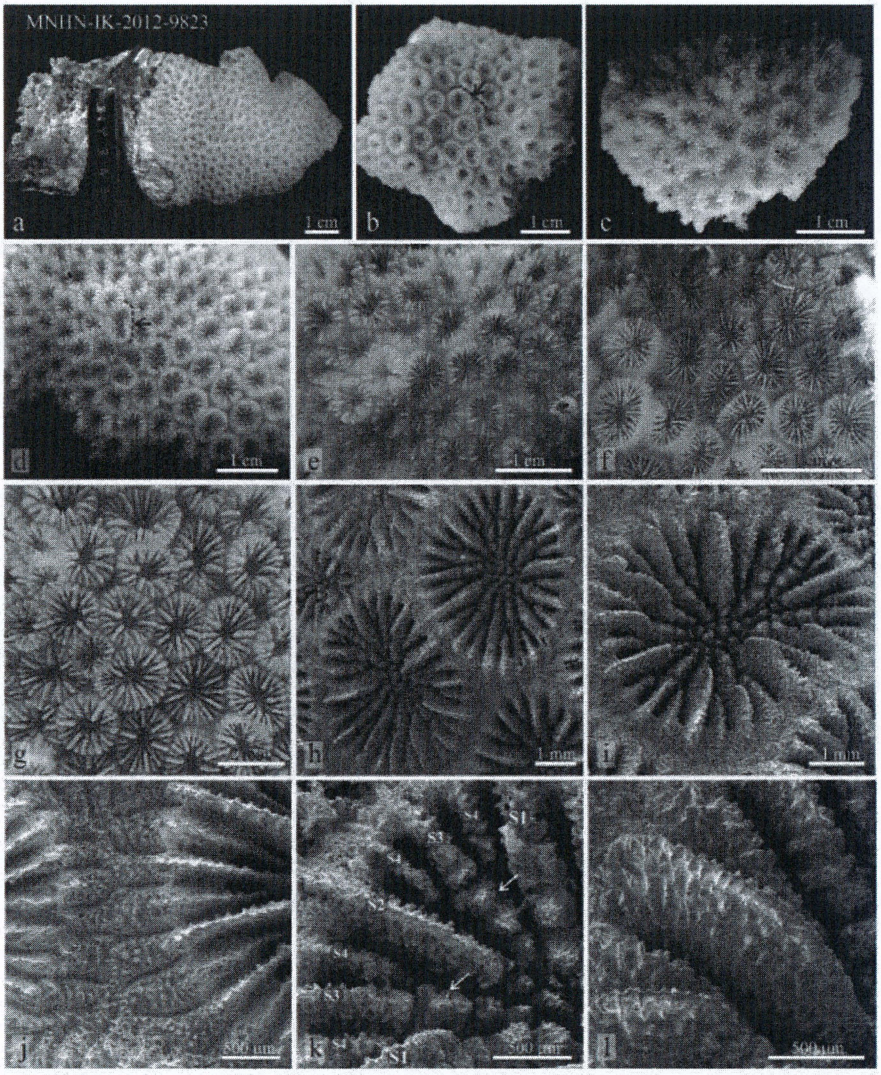

1107

1108 **Fig. 4** Maximum Likelihood (ML) phylogenetic tree of *Leptastrea* estimated with RAxML v8.2.10 using **a** the

1109 concatenated "holobiont-max" supermatrix (3,701 loci including a total of 44,162 SNPs); **b** the concatenated "coral-

1110 max" supermatrix (9,573 loci including a total of 62,728 SNPs). Branch support is based on ML bootstrap analyses ≥

1111 50 (first number at node) and Bayesian posterior probabilities ≥ 0.5 (second number at node)

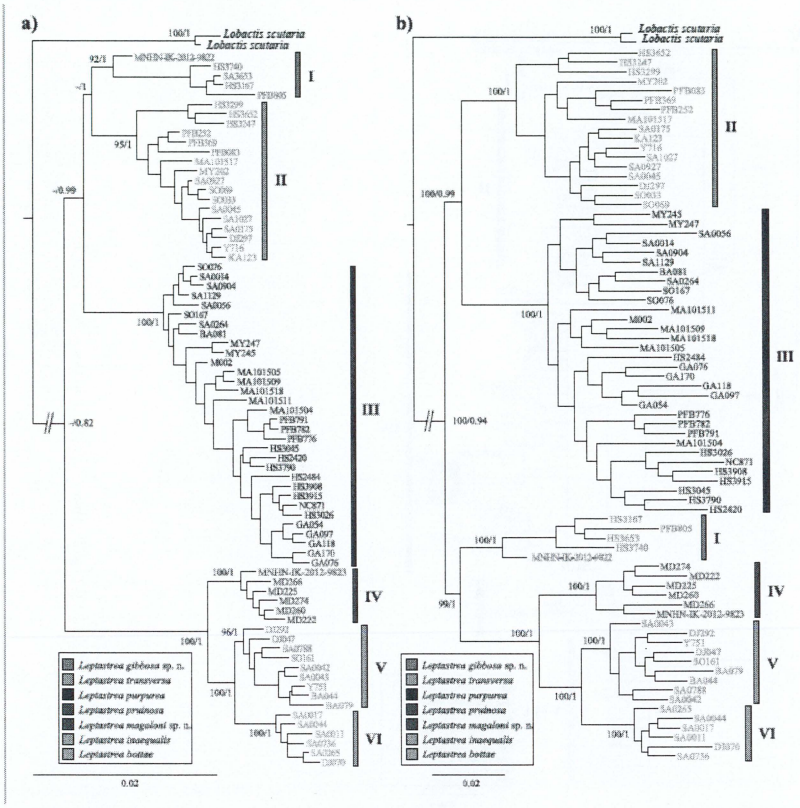

1112

1113 **Fig. 5** Maximum Likelihood (ML) phylogenetic tree of *Leptastrea* estimated with RAxML v8.2.10 using **a** nearly
1114 complete coral mitochondrial genomes (10,837 bp); **b** nearly complete nuclear ribosomal DNA arrays (5,835 bp).
1115 Branch support is based on ML bootstrap analyses ≥ 50 (first number at node) and Bayesian posterior probabilities ≥
1116 0.5 (second number at node)

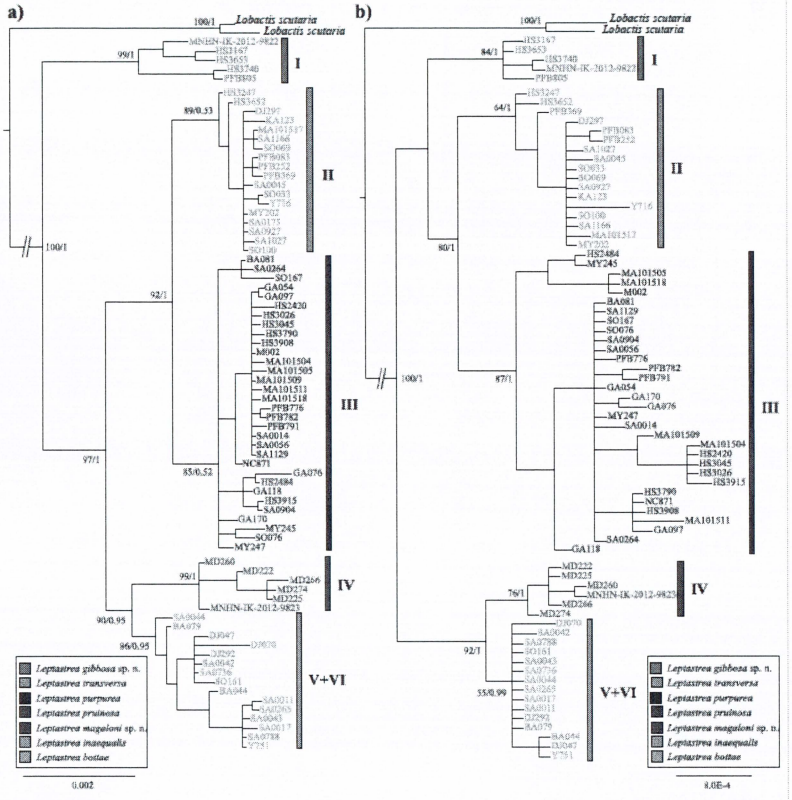

Fig. 6 Species tree estimation of *Leptastrea* based on 1,857 unlinked biallelic SNPs with 0% missing data inferred from SNAPP, following the best-supported model from the Bayes Factor Delimitation with genomic data (BFD*) analysis shown in Table 1. **a** complete set of consensus trees visualized with DensiTree; **b** distribution maps of each species. Circles denote specimens analyzed in this study, squares specimens deposited at museum collections that we identified based on our newly proposed morphological treatment, stars type locality

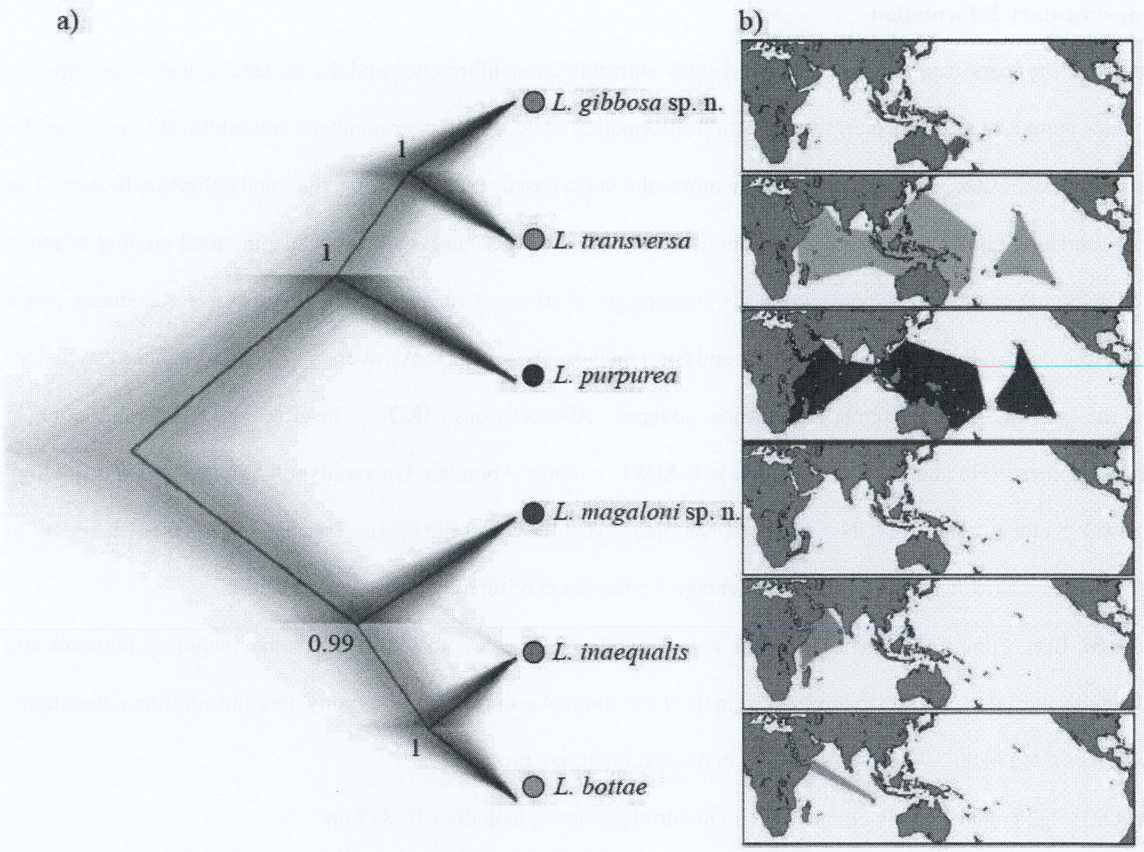

1123

1124 **Fig. 7** Plot of the first two principal components (PC) analyses of all examined *Leptastrea* specimens including
1125 holotypes (star symbols), showing the ordination of the specimens based on corallite morphometric variables. Each
1126 symbol represents a specimen (average of 5 replicates). Groups of specimens of the same species are enclosed by
1127 dashed polygon. Corresponding genetic clade in parenthesis as per Fig. 4. Color code is the same as in Figs. 4-6

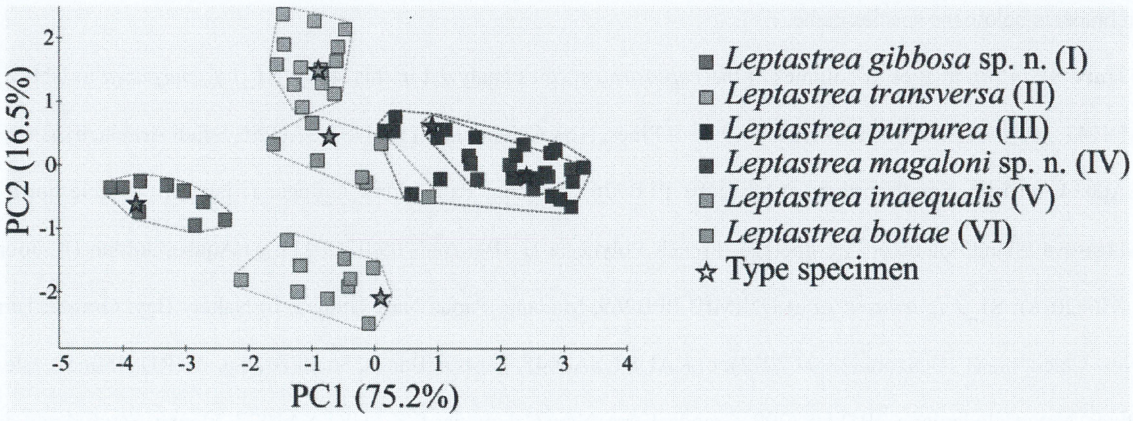

1128

1129

Supplementary Information

Data S1 List of coral samples analyzed in this study with collection information and the sequencing and bioinformatics statistics summary. In particular, the collection information includes voucher numbers, museum/institute where the specimen is deposited, species identification, molecular clade based on SNPs phylogenies, and collection locality. The sequencing and bioinformatics statistics summary includes the total number of raw reads, the total number of reads after trimming and relative percentage, the percentage of trimmed reads mapped to reference sequences (coral transcriptome, coral mitochondrial genome, and coral nuclear ribosomal DNA), average deviation, standard deviation, and the percentage of reference sequence covered. Abbreviations: IRD = Institute de Recherche pour le Développement (Noumea, New Caledonia); KAUST = King Abdullah University of Science and Technology (Thuwal, Saudi Arabia); MNHN = Muséum National d'Histoire Naturelle (Paris, France); UNIMIB = University of Milano-Bicocca (Milan, Italy); refseq_percentage = percentage of reference sequence covered.

Data S2 List of the *Leptastrea* specimens examined for the species treated in this study including museum and collected material in addition to those listed in the Taxonomic Account. Species synonymies and additional taxonomic references cited in the synonymies, but not in the main text, are provided.

Data S3 Alignment of nearly complete mitochondrial genomes, including 10,837 bp.

Data S4 Alignment of nearly complete nuclear ribosomal DNA regions, including 5,835 bp.

Data S5 Average (st. dev.) values of the six *Leptastrea* skeleton variables measured in this study: v1, maximum calice diameter; v2, minimum calice diameter; v3, maximum columella diameter; v4, minimum columella diameter perpendicular to v3; v5, distance between the centre of the columella and the centre of the columella of the closest adjacent corallite; v6, width of the groove among the corallites. The number of coralla examined per species is given in brackets below the species name.

Figure S1 *In situ* images of colonies of the *Leptastrea* species analyzed in this study: S1_1 *L. purpurea* a) UNIMIB MY143, Mayotte Island; b) IRD HS3790, Isle of Pines, New Caledonia; c) KAUST SA0056, Saudi Arabia; d) KAUST SA0014, Al Lith, Saudi Arabia; e) UNIMIB PFB776, Kavieng, Papua New Guinea; f) lagoon pinnacle north of Magareva Island, Gambier Archipelago, French Polynesia (F. Benzoni, 05/07/2011); g) Aqaba, Jordan (R. Joury, 17/07/2018); S1_2 *L. transversa* a) UNIMIB PFB369, Madang, Papua New Guinea; b) Nakety Bay, Grande Terre, New Caledonia (F. Benzoni, 22/04/2012); c) KAUST SA0045, Farasan Banks, Saudi Arabia; d) IRD HS3652, Isle of Pines, New Caledonia; e) IRD HS3299, Grande Terre, New Caledonia; f) KAUST SA1027, Magna, Saudi Arabia; g)

Aqaba, Jordan (R. Joury, 17/07/2018); S1_3 *L. bottae* a) KAUST SA0736 Ras Al-Ubayd, Saudi Arabia; b) KAUST SA0011, Al Lith, Saudi Arabia; c) Aqaba, Jordan (F. Benzoni, 09/07/2018); d) KAUST SA0044, Farasan Banks, Saudi Arabia; e) UNIMIB DJ070, Oblal, Djibouti; f) KAUST SA0011, Al Lith, Saudi Arabia; g) Aqaba, Jordan (R. Joury, 16/07/2018); S1_4 *L. inaequalis* a) UNIMIB BA079, Bir Ali, Yemen; b) UNIMIB DJ047, Oblal, Djibouti; c) Aqaba, Jordan (F. Benzoni, 15/07/2018); d) KAUST SA0043, Farasan Banks, Saudi Arabia; e) KAUST SA0042, Farasan Banks, Saudi Arabia; f) Socotra Island, Yemen (F. Benzoni, 18/03/2010); g) Aqaba, Jordan (R. Joury, 16/07/2018); S1_5 *Leptastrea gibbosa* sp. n. a) Lifou Island, Loyalty Islands, New Caledonia (F. Benzoni, 18/02/2014); b) outer reef south of the Grande Terre, New Caledonia (F. Benzoni, 08/11/2017); c) IRD HS3167, Moneo, Grande Terre, New Caledonia; d) UNIMIB PFB805, Kavieng, Papua New Guinea; e) IRD HS3740, Isle of Pines, New Caledonia; f) IRD HS3653, Isle of Pines, New Caledonia ; g) Mellish Reef, Australia (F. Benzoni, 02/12/2018); S1_6 *Leptastrea magaloni* sp. n. a) IRD MD266, Nosy Sakatia, Madagascar; b) IRD MD260, Nosy Be, Madagascar; c) IRD MD222, Nosy Lava, Madagascar; d) MNHN-IK-2012-9823, Bouzi, Mayotte Island; e) IRD MD225, Nosy Lava, Madagascar; f) IRD MD183, Nosy Mitsio, Madagascar; g) IRD MD274, Nosy Sakatia, Madagascar; h) same colony as in g with retracted tentacles. All *in situ* specimen images by F. Benzoni. For specimens, site and date metadata can be found in Data S1.

Figure S2 Maximum Likelihood (ML) phylogenetic tree of *Leptastrea* estimated with RAxML v8.2.10 using a) the concatenated "holobiont-min" supermatrix (2,075 loci including a total of 2,141 SNPs); b) the concatenated "coral-min" supermatrix (2,366 loci including a total of 2,479 SNPs). Branch support is based on ML bootstrap analyses.

Figure S3 Maximum Likelihood (ML) phylogenetic tree of *Leptastrea* estimated with RAxML v8.2.10 using a) the barcoding portion of the cytochrome oxidase subunit I gene of the mitochondrial genome (COI); b) the complete ITS1, 5.8S, and ITS2 regions of the nuclear ribosomal DNA (ITS). Branch support is based on ML bootstrap analyses.

Figure S4 Variability of skeleton morphology across specimens of the *Leptastrea* species examined in this study included in the genomic and morphometric analyses: *L. purpurea* (a-h), *L. transversa* (i-l), *L. gibbosa* sp. n. (m-p), *L. inaequalis* (q-t), *L. bottae* (u-x), *L. magaloni* sp. n. (y-ab). a) UNIMIB BA081; b) UNIMIB MY247; c) UNIMIB MY245; d) IRD HS3045; e) UNIMIB PFB776; f) UNIMIB GA097; g) UNIMIB GA170; h) UNIMIB GA076; i) UNIMIB DJ297; j) UNIMIB MY202; k) UNIMIB PFB252; l) IRD HS3247; m) UNIMIB PFB805; n) IRD HS3740; o and p) IRD HS2344; q) UNIMIB DJ292; r) UNIMIB BA044; s) UNIMIB BA079; t) UNIMIB DJ047; u) UNIMIB AD040; v) UNIMIB DJ070; w) UNIMIB BAL144; x) UNIMIB DJ335; y) UNIMIB MY333; z) IRD MD260; aa) IRD

1186 MD183; ab) IRD MD222. All images were taken at the same magnification (scale bar shown in a). Colour code same
1187 as in Figures 4-7. Collection metadata for *L. magaloni* sp. n. and *L. gibbosa* sp. n. specimens are in the Taxonomic
1188 Account, for all the other species in Data S1.